

HAGI++: Head-Assisted Gaze Imputation and Generation

CHUHAN JIAO, University of Stuttgart, Germany

ZHIMING HU, The Hong Kong University of Science and Technology (Guangzhou), China

ANDREAS BULLING, University of Stuttgart, Germany

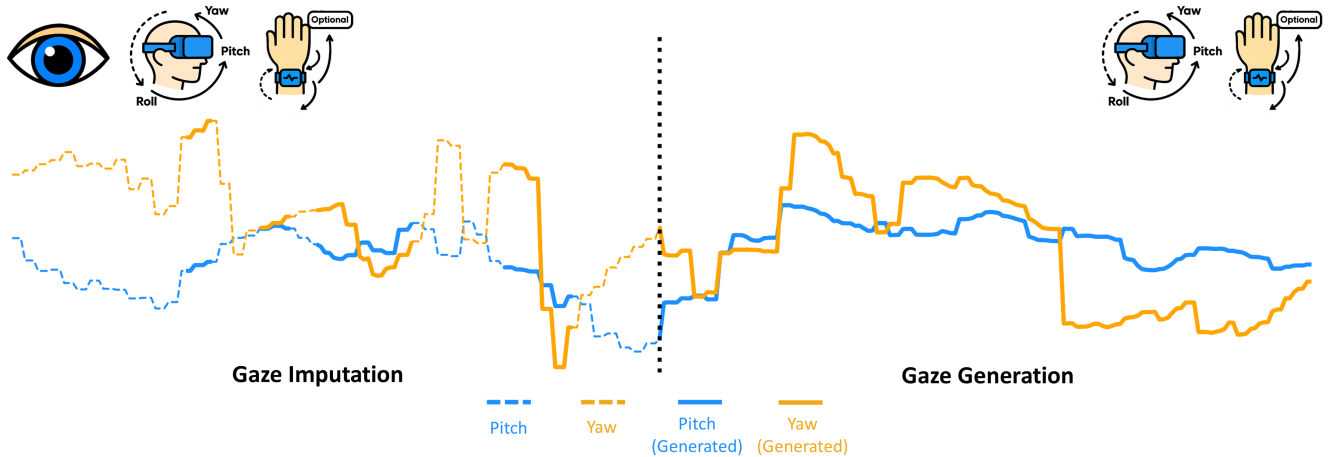


Fig. 1. Missing data is inevitable in mobile eye tracking. HAGI++ is a novel multi-modal diffusion model for gaze data imputation that leverages the close coordination between eye and head movements. The input to our method comprises gaze data with missing values and time-aligned head movements captured by sensors readily available in mobile eye trackers (left). For XR headsets without built-in eye tracking, HAGI++ can generate gaze data directly from head movements (right). Furthermore, when wrist or hand motion data from commodity wearable devices are available, HAGI++ can be easily extended to exploit eye–hand–head coordination for both tasks. HAGI++ achieves lower mean angular error and produces more realistic gaze trajectories than previous methods.

Mobile eye tracking plays a vital role in capturing human visual attention across both real-world and extended reality (XR) environments, making it an essential tool for applications ranging from behavioural research to human-computer interaction. However, missing values due to blinks, pupil detection errors, or illumination changes pose significant challenges for further gaze data analysis. To address this challenge, we introduce HAGI++ – a multi-modal diffusion-based approach for gaze data imputation that, for the first time, uses the integrated head orientation sensors to exploit the inherent correlation between head and eye movements. HAGI++ employs a transformer-based diffusion model to learn cross-modal dependencies between eye and head representations and can be readily extended to incorporate additional body movements. Extensive evaluations on the large-scale Nymeria, Ego-Exo4D, and HOT3D datasets demonstrate that HAGI++ consistently outperforms conventional interpolation methods and deep learning-based time-series imputation baselines in gaze imputation. Furthermore, statistical analyses confirm that HAGI++ produces gaze velocity distributions that closely match actual human gaze behaviour, ensuring more realistic gaze imputations. Moreover, by incorporating wrist motion captured from commercial wearable devices, HAGI++ surpasses prior methods that rely on full-body motion capture in the extreme case of 100% missing gaze data (pure gaze generation). Our method paves the way for more complete and accurate eye gaze recordings in real-world settings and has significant potential for enhancing gaze-based analysis and interaction across various application domains.

1 INTRODUCTION

Mobile eye tracking has become an essential tool for studying human behaviour [Hu et al. 2023; Steil and Bulling 2015], attention [Müller et al. 2019; Qu et al. 2024], cognition [Kiefer et al. 2017; López et al. 2024], and decision-making processes [Kiefer et al. 2017; Wisiecka et al. 2023], and has emerged as an attractive modality for interaction in real-world environments [Kwok et al. 2019; Lystbæk et al. 2024, 2022; Turkmen et al. 2024]. Also, latest commercial head-mounted extended reality (XR) devices, such as the Apple Vision Pro [Apple Inc. 2023], Meta Quest Pro [Meta Platforms Inc. 2022], Microsoft HoloLens 2 [Microsoft Corporation 2019], and Project Aria Glasses [Engel et al. 2023] are equipped with integrated eye tracking functionality.

A fundamental challenge in working with gaze data recorded using mobile eye trackers is the prevalence of missing values arising from blinks, pupil detection failures, occlusions, or illumination changes [Blignaut and Wium 2014; Nyström et al. 2013, 2025]. Missing values can significantly degrade data quality and, in the worst case, render gaze recordings unusable for further analysis and downstream applications [Grootjen et al. 2023]. Prior research has largely adopted two strategies to address this issue: discarding missing values entirely [Ishii et al. 2013; Jiao et al. 2023; Nakano and Ishii 2010] or imputing them using interpolation methods, such as linear [Aracena et al. 2015; Bulling et al. 2008; Huang and Bulling 2019; Mannaru et al. 2017] or nearest neighbour interpolation [Zheng et al.

CCS Concepts: • **Computing methodologies** → **Artificial intelligence; Machine learning**; • **Human-centered computing**;

2022]. While discarding data ensures data integrity, it results in discontinuities, making gaze data unsuitable for applications requiring temporal completeness and consistency, such as for training machine learning models [Hu et al. 2021, 2023, 2020]. Data imputation preserves continuity but fails to accurately reconstruct naturalistic gaze trajectories or match the velocity profile of real human eye movements [Grootjen et al. 2023; Mannaru et al. 2017]. As such, none of these existing approaches is fully satisfying and there remains a critical need for advanced gaze imputation techniques that can handle missing gaze data in a robust, continuity-preserving, and biologically plausible manner.

We introduce HAGI++ – a novel multi-modal approach that leverages the close coordination between eye and head movements (also known as eye-head coordination) for gaze imputation. Our method exploits the fact that along with gaze data, the latest mobile eye trackers and XR headsets are also readily equipped with sensors for head tracking, such as inertial sensors or vision-based approaches for self-localisation and mapping. Unlike prior methods that treat gaze as a standalone signal, HAGI++ is the first to integrate head movement information to infer missing gaze values. In addition, recent mobile eye trackers and XR systems are increasingly paired with wearable devices such as controllers or wristbands, which capture hand or wrist movements for multi-modal interaction based on natural eye-hand coordination. HAGI++ is readily extensible to such inputs, allowing us to exploit eye-head-hand coordination for gaze imputation. Specifically, we introduce (1) HAGI++ as a transformer-based diffusion model that captures cross-modal dependencies between eye and head representations, and can be naturally extended to include further body movements (e.g., wrists), thereby exploiting broader eye-body coordination; (2) we propose a hybrid feature-fusion mechanism based on FiLM (feature-wise linear modulation) [Perez et al. 2018] that effectively combines head, gaze, and other body motion features across multiple levels.

We evaluate HAGI++ on head-assisted gaze imputation on three large-scale gaze datasets that cover different everyday indoor and outdoor activities: Nymeria [Ma et al. 2024], Ego-Exo4D [Grauman et al. 2024], and HOT3D [Banerjee et al. 2024]. Results of these evaluations show that our approach significantly outperforms both interpolation-based methods and deep learning-based time-series imputation baselines. Our method reduces mean angular error (MAE) by up to 25.3%, and yields gaze velocity distributions that more closely resemble real human gaze movements than other methods. Furthermore, using the wrist-movement signals available in Nymeria, we demonstrate that incorporating wrist movements further improves gaze imputation in high data-loss scenarios and achieves performance on par with head-only input under low data-loss conditions. Finally, we evaluate HAGI++ under the extreme setting of 100% gaze data loss (pure gaze generation). Remarkably, with only commodity wearable inputs, HAGI++ outperforms the previous state-of-the-art [Hu et al. 2024b]—which requires full-body motion capture—by 17.6% on the Nymeria dataset.

Our main contributions are as follows:

- (1) We introduce HAGI++, the first multi-modal diffusion-based approach for gaze imputation that exploits the coordination between eye and head movements.
 - (2) We conduct extensive evaluations on three large-scale egocentric gaze datasets, demonstrating that HAGI++ outperforms existing methods—achieving up to a 25.3% reduction in mean angular error—and generates gaze velocity distributions that closely resemble real human gaze dynamics, ensuring more naturalistic and biologically plausible imputed gaze trajectories.
 - (3) We extend HAGI++ to incorporate wrist movements, captured by commodity wearable devices such as wristbands or controllers. Our experiments demonstrate that wrist features provide additional gains in high data-loss scenarios, further highlighting the adaptability of our framework to broader eye-body coordination.
 - (4) We evaluate HAGI++ under the extreme setting of 100% data loss (pure gaze generation). Remarkably, using only signals from commodity wearable devices, our method surpasses the previous state of the art—which requires full-body motion capture—by 17.6% on the Nymeria dataset.
- By explicitly modelling eye-head (and, when available, eye-head-hand) coordination, HAGI++ enables more reliable gaze-based analysis and interaction in mobile eye-tracking applications. Our approach enhances the quality of gaze data in real-world scenarios, making it particularly beneficial for applications in XR, behavioural research, and gaze-based human-computer interaction. Furthermore, by supporting plausible gaze data generation from commodity wearables, HAGI++ opens new opportunities for computer graphics and interactive systems where realistic gaze behaviour is a critical component.
- An earlier related work was published in UIST 2025 [Jiao et al. 2025a]. This paper substantially extends the prior version in several key aspects:
- (1) **New model architecture.** We introduce a novel architecture, HAGI++, which consistently outperforms HAGI [Jiao et al. 2025a] across all gaze imputation experiments. In addition to its improved accuracy, HAGI++ delivers faster inference, making it more efficient in computation.
 - (2) **Optional integration of wrist movement signals.** We further extend our framework to optionally incorporate wrist movement data from commodity wearables, if available. This extension demonstrates that, additional wrist signals can enhance robustness under severe data loss, highlighting the potential of multi-modal eye-hand-head coordination for gaze modelling.
 - (3) **Evaluation on gaze data generation.** We present new experiments in the extreme case of 100% missing gaze data.
 - (4) **Comprehensive ablation analysis.** We perform detailed ablation studies to quantify the individual contributions of head rotation, head translation, wrist rotation, and wrist translation to gaze imputation performance.

2 RELATED WORK

2.1 Gaze Imputation

The task of gaze imputation, which involves reconstructing missing values within recorded gaze data, remains an underexplored area of research. The predominant approach to handle missing values in most prior studies has been to exclude instances containing missing gaze data entirely [Abdrabou et al. 2021; Appel et al. 2019; Arefin

et al. 2022; Bekele et al. 2013; Gunawardena et al. 2019; Vrzakova et al. 2021]. Among the limited works that do address missing data, classical interpolation techniques have been the primary method of choice. Notably, Huang and Bulling [Huang and Bulling 2019] applied linear interpolation to fill gaps in gaze data lasting less than 50 milliseconds, while Mannaru et al. [Mannaru et al. 2017] similarly employed linear interpolation for recovering missing gaze data in time-domain analyses. Alternative interpolation methods, such as nearest neighbours interpolation [Zheng et al. 2022], unsupervised Expectation-Maximization algorithm [Li et al. 2020], have also been explored in this context. However, as emphasised by Grootjen et al. [Grootjen et al. 2023], interpolation methods often struggle to accurately replicate the velocity distribution of real gaze data. On the other hand, machine learning techniques have also been applied to gaze super-resolution - a special type of gaze imputation. Jiao et al. [Jiao et al. 2023] introduced SUPREYES, an implicit neural representation learning method for gaze super-resolution. However, it is important to note that SUPREYES primarily operates on low-resolution gaze data without any missing values, focusing on resolution enhancement rather than imputing missing data at arbitrary positions. In stark contrast to previous methods, HAGI++ can impute missing gaze data at any arbitrary location while preserving the natural dynamics of human gaze behaviour by closely mimicking the gaze velocity distribution.

2.2 Eye-head Coordination

Eye-head coordination refers to the coordinated movements between the eyes and the head and has been extensively investigated in the areas of cognitive science and human-centered computing. Specifically, Stahl studied the process of gaze shift and found that the amplitude of head movement is proportional to the amplitude of gaze shift [Stahl 1999]. Fang et al. investigated the gaze fixation process and revealed that eye-head coordination plays a significant role in visual cognitive processing [Fang et al. 2015]. Hu et al. analysed eye-head coordination in immersive virtual environments and discovered that human eye gaze positions are strongly correlated with head rotation velocities [Hu et al. 2025b, 2020, 2019]. Sidenmark et al. focused on the process of gaze shift in virtual reality and identified the coordination of eye, head, and body movements [Sidenmark and Gellersen 2019a]. Emery et al. studied the process of performing various tasks, e.g. reading, drawing, shooting, and object manipulation, in virtual environments and identified general eye, hand, and head coordination patterns [Emery et al. 2021]. Recently, inspired by the strong link between eye and head movements, researchers started to use both eye and head information in many applications and have achieved great success [Gandrud and Interrante 2016; Hu et al. 2024a,c; Kothari et al. 2020; Kytö et al. 2018; Sidenmark et al. 2020; Yan et al. 2024]. For example, Gandrud et al. predicted users' locomotion directions in virtual reality using their gaze directions and head orientations [Gandrud and Interrante 2016]. Sidenmark et al. [Sidenmark and Gellersen 2019b] and Kytö et al. [Kytö et al. 2018] employed users' eye and head movements in virtual reality to improve the accuracy of target selection. Kothari et al. classified eye gaze events, i.e. fixations, pursuits, and saccades, from the magnitudes of eye and head movements [Kothari et al. 2020]. Hu et

al. predicted eye fixations in the future using historical gaze positions and head rotation velocities [Hu et al. 2021] and proposed to recognise the task a user is performing from user's eye and head movements [Hu et al. 2023].

Despite the fact that both eye and head motions are beneficial for many applications, they have not been studied together for eye gaze imputation yet. And existing gaze prediction methods [Hu et al. 2021, 2019] cannot be directly applied to gaze imputation, since they are only able to predict future gaze, but imputation requires a bi-directional method (e.g., filling in the previous gaze samples according to the observation). To the best of our knowledge, we are the first to demonstrate that eye-head coordination can be successfully transferred to the task of gaze imputation and lead to significant performance gains.

2.3 Eye-hand Coordination

Eye-hand coordination refers to the ability to synchronise visual input with hand movements, enabling precise motor control guided by visual feedback [Johansson et al. 2001; Land et al. 1999]. This coordination plays a crucial role in both human perception and action and has been widely leveraged to design interactive techniques in XR environments [Bertrand and Chapman 2023; Hu et al. 2025a; Ren et al. 2024; Wang et al. 2024]. Beyond interaction design, eye-hand coordination has also been explored in gaze prediction. For example, Hu et al. [Hu et al. 2024b] analysed multiple datasets and demonstrated strong correlations between gaze directions and wrist movements across everyday activities, introducing Pose2Gaze, a model that predicts gaze direction from full-body poses. More recently, Hu et al. [Hu et al. 2025b] proposed HOIGaze, which leverages two-hand gestures and 3D object information to improve gaze prediction performance during hand-object interactions.

In stark contrast to these prior works that rely on motion capture systems for body or hand pose acquisition, HAGI++ utilises head movements from head-mounted devices and motion data from off-the-shelf wearable devices such as smartwatches and wristbands. HAGI++ achieves clear performance gains over previous state-of-the-art methods that depend on motion capture, demonstrating that meaningful eye-hand-head coordination can be effectively modelled using readily available consumer hardware.

2.4 Time-Series Imputation

Since gaze data can be represented as a time series, in theory, existing time-series imputation methods can be directly applied to gaze data imputation. Deep learning-based methods have been shown to outperform statistical approaches in prior time-series imputation studies. Existing methods explore various neural network architectures, including Convolutional Neural Networks (CNNs), Recurrent Neural Networks (RNNs), Transformers, and Multilayer Perceptrons (MLPs). For example, TimesNet [Wu et al. 2023] transforms the input time series into the frequency domain and processes it using a CNN model; BRITS [Cao et al. 2018] employs a bidirectional RNN to capture temporal patterns in time series data; iTransformer [Liu et al. 2024], Informer [Zhou et al. 2021], and Crossformer [Zhang and Yan 2023] utilise different attention mechanisms within Transformers to better model time-series dynamics; DLinear [Zeng et al. 2023]

applies MLPs for computationally efficient time-series imputation. Generative methods such as Variational Autoencoders (VAEs), Generative Adversarial Networks (GANs), and diffusion models have also been explored for time-series imputation, including US-GAN [Miao et al. 2021], GP-VAE [Fortuin et al. 2020], and CSDI [Tashiro et al. 2021].

While these methods offer powerful general-purpose solutions, they are typically designed for single-modal signals and do not account for the unique characteristics of gaze data or the availability of complementary head movement signals in mobile eye tracking. In contrast, HAGI++ is specifically tailored to the gaze imputation task and is, to our knowledge, the first to explicitly incorporate head movement information and other body movements captured by wearable devices as auxiliary modalities. Our approach is the first method that is specifically geared to the gaze imputation task and that leverages eye-hand (when available, eye-hand-head) coordination to enhance gaze imputation performance.

3 BACKGROUND

3.1 Gaze Data Imputation

Let $\mathbf{X} = \{x_1, x_2, \dots, x_L\} \in \mathbb{R}^{L \times K}$ be a sequence of gaze directions, where L represents the length of the gaze sequence, determined by the sampling rate of the eye tracker and the duration of data collection. In our case, we set $K = 2$, as each gaze direction at any given time step is represented by (pitch, yaw). Additionally, we define $\mathbf{M} = \{m_1, m_2, \dots, m_L\} \in \{0, 1\}^{L \times 1}$ to denote an observation mask, where $m_l = 1$ indicates that the eye tracker produces a valid output for x_l , while $m_l = 0$ denotes that x_l is invalid. Gaze data imputation is the task of estimating the gaze directions for invalid values within \mathbf{X} by leveraging the valid gaze observations in \mathbf{X} .

3.2 Conditional Score-based Diffusion Model for Time-Series Imputation (CSDI)

Denoising Diffusion Probabilistic Models (DDPMs) [Ho et al. 2020] are a class of generative models that have achieved state-of-the-art performance across a range of domains, including image generation [Ho et al. 2020], audio synthesis [Kong et al. 2021], and more recently, eye movement synthesis [Jiao et al. 2025b, 2024]. These models learn to generate realistic data by reversing a gradual noising process, enabling fine-grained control over the generative trajectory.

Tashiro et al. [Tashiro et al. 2021] extended the diffusion framework to time-series imputation by proposing Conditional Score-based Diffusion for Imputation (CSDI). CSDI models the conditional distribution of missing values given the observed portions of the time series. It introduces a conditional training scheme in which a masking function stochastically selects observed and unobserved regions of the input during training, allowing the model to learn flexible imputation strategies across various missing patterns.

Since gaze data is also time-series, CSDI can be adapted for gaze data imputation. CSDI is trained in a self-supervised manner. During training, given an input time series \mathbf{x}_0 , CSDI randomly generates an observation mask that separates \mathbf{x}_0 into the observed part \mathbf{x}_0^{co} and the target part requiring imputation \mathbf{x}_0^{ta} . As with the original DDPM, CSDI consists of two processes: The forward process is a Markov chain that progressively adds noise to \mathbf{x}_0^{ta} , to transform \mathbf{x}_0^{ta}

into random noise following a Gaussian distribution. The forward process is defined as follows:

$$q(\mathbf{x}_t^{ta} | \mathbf{x}_0^{ta}) = \mathcal{N}(\mathbf{x}_t^{ta}; \sqrt{\alpha_t} \mathbf{x}_0^{ta}, (1 - \alpha_t) I) \quad (1)$$

where t denotes the time step, and α_t is a constant determined by a predefined noise schedule. More specifically,

$$\mathbf{x}_t^{ta} = \sqrt{\alpha_t} \mathbf{x}_0^{ta} + (1 - \alpha_t) \epsilon \quad (2)$$

where $\epsilon \sim \mathcal{N}(0, I)$ is random Gaussian noise.

The reverse process aims to start from pure Gaussian noise, similar to \mathbf{x}_t^{ta} , and iteratively denoise it to reconstruct a sample resembling the original data distribution. Since, in imputation, we additionally have conditional information from the observed sequence \mathbf{x}_0^{co} , the reverse process is defined as follows:

$$p_\theta(\mathbf{x}_{t-1}^{ta} | \mathbf{x}_t^{ta}, \mathbf{x}_0^{co}) = \mathcal{N}(\mathbf{x}_{t-1}^{ta}; \mu_\theta(\mathbf{x}_t^{ta}, t | \mathbf{x}_0^{co}), \sigma_\theta(\mathbf{x}_t^{ta}, t | \mathbf{x}_0^{co}) I) \quad (3)$$

where θ represents the trainable parameters of the neural network,

$$\mu_\theta(\mathbf{x}_t^{ta}, t | \mathbf{x}_0^{co}) = \frac{1}{\alpha_t} \left(\mathbf{x}_t^{ta} - \frac{1 - \alpha_t}{\sqrt{1 - \alpha_t}} \epsilon_\theta(\mathbf{x}_t^{ta}, t | \mathbf{x}_0^{co}) \right), \quad (4)$$

and $\sigma_\theta(\mathbf{x}_t^{ta}, t | \mathbf{x}_0^{co}) I$ is a constant defined by the noise schedule. The term $\epsilon_\theta(\mathbf{x}_t^{ta}, t | \mathbf{x}_0^{co})$ in Equation 4 is a trainable denoising deep learning model. The training objective is to minimise the difference between the prediction and the actual added noise in Equation 2:

$$\mathcal{L}_{noise} = \|\epsilon_t - \epsilon_\theta(\mathbf{x}_t^{ta}, t | \mathbf{x}_0^{co})\|_2 \quad (5)$$

4 HEAD-ASSISTED CONDITIONAL DIFFUSION MODEL FOR GAZE IMPUTATION

Previous studies have demonstrated that human eye movements are strongly correlated with head movements, a phenomenon known as eye-head coordination [Emery et al. 2021; Hu et al. 2023, 2019; Sidenmark and Gellersen 2019a,b; Stahl 1999]. Most commercially available head-mounted devices equipped with eye-tracking capabilities, such as the Apple Vision Pro [Apple Inc. 2023], Meta Quest Pro [Meta Platforms Inc. 2022], Microsoft HoloLens 2 [Microsoft Corporation 2019], or Project Aria Glasses [Engel et al. 2023], are readily fitted with sensors for tracking users' head movements. Unlike gaze data, which inevitably contains missing values [Grootjen et al. 2024b; Nyström et al. 2025], head movements are recorded continuously without any missing data, provided the sensor remains operational. The key idea of HAGI++ is to exploit the close coordination between head and eye movements to impute missing values in gaze data. At its core, HAGI++ employs a transformer-based diffusion model conditioned on observed gaze data and time-aligned head motion, enabling accurate and realistic gaze imputation. Beyond head signals, the framework is designed to incorporate additional wrist movements, captured from commodity wearable devices such as smartwatches, wristbands, or XR hand controllers. This extension exploits natural eye-hand coordination [Binsted et al. 2001; Johansson et al. 2001] to further enhance imputation performance (see Section 4.2 and 4.3). Moreover, HAGI++ generalises to the extreme case of gaze generation (i.e., 100% missing data), where it synthesises realistic gaze trajectories conditioned solely on head and auxiliary body movements captured by wearable sensors.

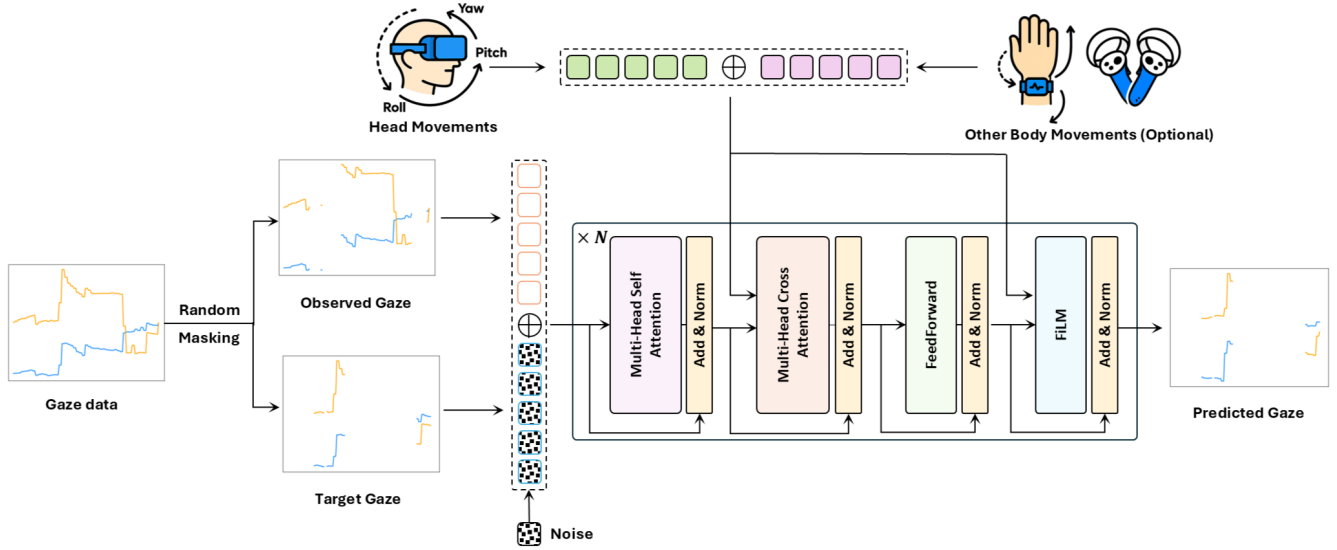


Fig. 2. Overview of the training pipeline and model architecture of HAGI++. During training, a complete gaze sequence is divided into an observed segment and a target segment. The objective of HAGI++ is to reconstruct the target gaze sequence from the observed gaze, time-aligned head movements, and optionally, other body movements (e.g., wrist motions) captured by commodity wearable devices. All input modalities are projected into token representations via MLPs. The core of HAGI++ consists of a stack of N transformer blocks. Each block contains a self-attention layer that captures correlations between the concatenated observed and noisy gaze tokens, a cross-attention layer that models eye-head or eye-hand-head coordination, and a FiLM layer that further integrates movement features for gaze prediction. HAGI++ can be readily adapted for gaze generation by removing the observed gaze input. This design enables HAGI++ to effectively capture multimodal eye-head or eye-hand-head coordination for accurate and realistic gaze imputation and generation.

4.1 Problem Definition and Data Preparation

Head-assisted gaze imputation. We extend the definition of gaze data imputation outlined in Section 3.1. For each gaze sequence $\mathbf{X} = \{x_1, x_2, \dots, x_L\}$, we have a corresponding sequence of time-aligned head movements $\mathbf{H} = \{h_1, h_2, \dots, h_L\}$ captured by the head-mounted eye trackers. The task is to predict the gaze directions for missing values within \mathbf{X} by leveraging both the head movements \mathbf{H} and the existing gaze observations in \mathbf{X} . Since head movements correspond to the movements of head-mounted devices, we obtain \mathbf{H} by processing the SLAM poses of the head-mounted device. Let us denote $T_{\text{world, tracker}}^l \in SE(3)$ as the pose of the mobile eye tracker in the world coordinate system at time step l . The head movement at time step l is represented as the relative transformation matrix between the SLAM poses at two consecutive time steps:

$$h_l = \Delta T_{\text{tracker}}^{l,l+1} = (T_{\text{world, tracker}}^l)^{-1} T_{\text{world, tracker}}^{l+1} \quad (6)$$

For each gaze sample x_l , represented as (pitch, yaw), we normalise the values to the range $[0, 1]$ using a sine transformation before further processing.

Extension to wrist/hand movements. When additional time-aligned signals from wrist-worn or hand-held devices (e.g., smartwatches, wristbands, or XR controllers) are available, the definition naturally extends to include an auxiliary modality $\mathbf{W} = \{w_1, w_2, \dots, w_L\}$ of wrist/hand movements. Since both gaze and head are represented in the tracker-centric coordinate system, we express wrist motion at time step l relative to the eye tracker. For example, consider a smart

wristband worn on the left hand, with pose $T_{\text{world, band}}^l \in SE(3)$ at time step l . The relative transformation is then defined as:

$$w_l = T_{\text{tracker, band}}^l = (T_{\text{world, tracker}}^l)^{-1} T_{\text{world, band}}^l. \quad (7)$$

This formulation allows HAGI++ to exploit eye-head-hand coordination for gaze imputation.

4.2 HAGI++ Diffusion Process

At the core of HAGI++ lies a conditional diffusion model that performs gaze imputation by exploiting the strong correlations between eye and head movements, and optionally wrist movements when available. Although diffusion models have recently demonstrated strong performance in general time-series imputation tasks (Section 3.2), they have not yet been adapted to handle multi-modal signals that exhibit biomechanical coordination, such as the coupled dynamics of gaze and head motion.

To this end, we design a body-movement-conditioned diffusion framework that seamlessly integrates body movements—most notably head movements—throughout the denoising process. These movements can be readily captured using commodity wearable devices, enabling practical deployment in real-world scenarios. Let x_0 denote the input gaze sequence, with x_0^{o} and $x_0^{t_a}$ representing the observed and target parts, respectively, separated by a randomly generated binary observation mask. The forward diffusion process in HAGI++ follows the same formulation as CSDI [Tashiro et al. 2021]. Given \mathbf{B} as the sequence of head and other body movements

Algorithm 1 HAGI++ Training Procedure

```

1: Input: gaze data  $\mathbf{X}$ , corresponding head movements and other
   available body movements  $\mathbf{B}$ , total diffusion step  $T$ 
2: repeat
3:    $\mathbf{x}_0 = \sin(\mathbf{X})$ 
4:    $\mathbf{M} \sim \text{Random Mask Generator}$ 
5:    $\mathbf{x}_0^{co} = \mathbf{M} \odot \mathbf{x}_0$ 
6:    $\mathbf{x}_0^{ta} = (1 - \mathbf{M}) \odot \mathbf{x}_0$ 
7:    $t \sim \text{Uniform}(\{1, \dots, T\})$ 
8:    $\epsilon \sim \mathcal{N}(0, I)$ 
9:    $\mathbf{x}_t^{ta} = \sqrt{\alpha_t} \mathbf{x}_0^{ta} + (1 - \alpha_t) \epsilon$ 
10:   $\mathcal{L} = \|\epsilon_t - \epsilon_\theta(\mathbf{x}_t^{ta}, t \mid \mathbf{x}_0^{co}, \mathbf{B})\|_2$ 
11:   $\nabla_\theta \mathcal{L}$ 
12: until converged

```

captured by wearable sensors, corresponding to \mathbf{x}_0 , the reverse process of HAGI++ extends Equation 3 as follows:

$$p_\theta(\mathbf{x}_{t-1}^{ta} \mid \mathbf{x}_t^{ta}, \mathbf{x}_0^{co}, \mathbf{B}) = \mathcal{N}(\mathbf{x}_{t-1}^{ta}; \mu_\theta(\mathbf{x}_t^{ta}, t \mid \mathbf{x}_0^{co}, \mathbf{B}), \sigma_\theta(\mathbf{x}_t^{ta}, t \mid \mathbf{x}_0^{co}, \mathbf{B})) \quad (8)$$

As with standard denoising diffusion models [Ho et al. 2020; Hu et al. 2025c; Kong et al. 2021; Shi et al. 2025; Tashiro et al. 2021; Zhang et al. 2024b], the training objective of HAGI++ is to accurately predict the added noise at diffusion time step t :

$$\mathcal{L} = \|\epsilon_t - \epsilon_\theta(\mathbf{x}_t^{ta}, t \mid \mathbf{x}_0^{co}, \mathbf{B})\|_2 \quad (9)$$

Figure 2 shows the HAGI++ training pipeline. Algorithm 1 and Algorithm 2 summarise HAGI++’s training and sampling procedures.

Algorithm 2 HAGI++ Sampling Procedure

```

1: Input: gaze data  $\mathbf{X}$ , corresponding head movements and other
   available body movements  $\mathbf{B}$ , observation mask  $\mathbf{M}$ 
2:  $\mathbf{x}_0^{co} = \mathbf{M} \odot \sin(\mathbf{X})$ 
3: Sample  $\mathbf{x}_T^{ta} \sim \mathcal{N}(0, I)$ 
4: for  $t = T, T - 1, \dots, 1$  do
5:    $\mu_\theta(\mathbf{x}_t^{ta}, t \mid \mathbf{x}_0^{co}, \mathbf{B}) = \frac{1}{\alpha_t} \left( \mathbf{x}_t^{ta} - \frac{1 - \alpha_t}{\sqrt{1 - \alpha_t}} \epsilon_\theta(\mathbf{x}_t^{ta}, t \mid \mathbf{x}_0^{co}, \mathbf{B}) \right)$ 
6:   Sample  $\mathbf{x}_{t-1}^{ta} \sim p_\theta(\mathbf{x}_{t-1}^{ta} \mid \mathbf{x}_t^{ta}, \mathbf{x}_0^{co}, \mathbf{B})$  using Equation 8
7: end for
8: Output:  $\arcsin(\mathbf{x}_0^{ta})$ 

```

4.3 HAGI++ Architecture

Figure 2 shows an overview of the HAGI++ architecture. The primary challenge lies in effectively integrating information from head movements—and other body movements captured by commodity wearable devices—with the observed gaze sequence \mathbf{x}_0^{co} to accurately reconstruct the missing gaze samples \mathbf{x}_0^{ta} . To this end, we design a transformer-based diffusion model that captures cross-modal dependencies between eye and head representations, and can be naturally extended to include additional body movements (e.g., wrist motions) to exploit broader eye–body coordination. Furthermore, we introduce a hybrid feature fusion mechanism leveraging stylisation blocks that combine body-movement and gaze features

across multiple levels to further improve the performance. This design enables HAGI++ to learn a more coherent correlation between head and gaze dynamics, leading to more accurate and realistic gaze imputation.

Input mapping. As outlined in Sections 3.1 and 4.1, the input gaze data is represented as a sequence of (pitch, yaw) with shape $(L, 2)$, where L denotes the sequence length. The input gaze data is then divided into the observed gaze $\mathbf{x}_0^{co} \in \mathbb{R}^{L \times 2}$ and the noisy target part $\mathbf{x}_t^{ta} \in \mathbb{R}^{L \times 2}$ using a randomly generated mask and noise addition, as described in Algorithm 1.

The head movements captured by the mobile eye tracker are denoted as $\mathbf{H} \in \mathbb{R}^{L \times 4 \times 3}$, consisting of a sequence of transformations $h_t = [R, \mathbf{t}] \in \mathbb{R}^{4 \times 3}$, where $R \in \mathbb{R}^{3 \times 3}$ represents head rotation and $\mathbf{t} \in \mathbb{R}^{1 \times 3}$ corresponds to head translation. Following established practice for processing transformation matrices [Yi et al. 2024], each transformation is first flattened into a 12-dimensional vector, after which we apply Fourier positional encoding to obtain the encoded head movements $\mathbf{H} \in \mathbb{R}^{L \times 12}$.

When additional body movements—such as wrist or hand movements $\mathbf{W} \in \mathbb{R}^{L \times 4 \times 3}$, as introduced in Section 4.1—are available, we apply the same Fourier encoding to \mathbf{W} .

For each input modality, including the binary observation mask \mathbf{M} , we project the features into a shared latent space of dimension $D = 64$ using a multilayer perceptron (MLP) followed by a GELU activation. To preserve temporal order, sinusoidal positional encodings [Vaswani et al. 2017] of shape (L, D) are added to each projected sequence, except for the observation mask. The noisy and observed gaze features are then concatenated along the feature dimension to form a unified gaze tensor $\mathbf{G} \in \mathbb{R}^{L \times 2D}$. Finally, the projected head features, conditional mask, and—when available—other body-movement features are concatenated along the feature dimension to form a unified motion context tensor $\mathbf{B} \in \mathbb{R}^{L \times D_{\text{motion}}}$, where $D_{\text{motion}} = N_{\text{motion}} \times D$ and N_{motion} denotes the number of conditional modalities. This motion context serves as auxiliary input to guide the gaze imputation process.

Transformer block. At the core of the HAGI++ architecture lies a stack of N transformer blocks. In each block, we first map the diffusion step t to the same dimension as the gaze tensor \mathbf{G} and merge it via element-wise addition, enabling the model to adapt its denoising behaviour according to the current diffusion timestep.

Within-gaze correlation. We begin by applying a self-attention mechanism to the gaze tensor to capture temporal dependencies and spatial relationships between the observed and missing gaze samples. Specifically, the gaze tensor is refined as:

$$\mathbf{G} = \mathbf{G} + \text{softmax}\left(\frac{\mathbf{Q}\mathbf{K}^\top}{\sqrt{2D}}\right) \mathbf{V}, \quad (10)$$

where $\mathbf{Q} = \text{LN}(\mathbf{G})W^Q$, $\mathbf{K} = \text{LN}(\mathbf{G})W^K$, and $\mathbf{V} = \text{LN}(\mathbf{G})W^V \in \mathbb{R}^{L \times 2D}$ denote the queries, keys, and values obtained through learnable projection matrices W^Q , W^K , and W^V , respectively. Here, $\text{LN}(\cdot)$ represents Layer Normalisation [Ba et al. 2016], which stabilises training and improves feature consistency across timesteps.

Cross-modality correlation. Since prior work has shown that cross-attention effectively captures relationships between different modalities [Hu et al. 2025b], we introduce a cross-attention layer to model the coordination between gaze and body movements (e.g., head, wrist, or hand). This mechanism allows the model to dynamically attend to the most relevant motion cues at each timestep, thereby fusing multimodal information for more accurate gaze imputation. Formally, the gaze tensor is updated as:

$$\mathbf{G} = \mathbf{G} + \text{softmax}\left(\frac{\mathbf{Q}\mathbf{K}^\top}{\sqrt{D_{\text{motion}}}}\right)\mathbf{V}, \quad (11)$$

where $\mathbf{Q} = \text{LN}(\mathbf{G})W^Q \in \mathbb{R}^{L \times 2D}$, and $\mathbf{K} = \text{LN}(\mathbf{B})W^K$, $\mathbf{V} = \text{LN}(\mathbf{B})W^V \in \mathbb{R}^{L \times D_{\text{motion}}}$ are the key and value projections of the motion context tensor \mathbf{B} .

Similar to a standard Transformer [Vaswani et al. 2017], the attended features are further refined by a feed-forward network with GELU activation.

Hybrid fusion mechanism. Information from head and other body movements can degrade as it propagates through successive linear and nonlinear transformations within the feed-forward network. To mitigate this degradation, inspired by the skip connections in ResNet [He et al. 2016], we introduce a *skip fusion* mechanism that re-injects motion information at each Transformer block via feature-wise linear modulation (FiLM) [Perez et al. 2018]. This design allows the model to continuously fuse the auxiliary motion context with the gaze representation, ensuring that eye-head/body coordination remains effectively encoded throughout the denoising process.

Specifically, after the input mapping stage, we apply mean pooling to the encoded head features and any available body-movement features, concatenating them to form a global context vector denoted as \mathbf{C} . This context vector is input to each Transformer block to provide FiLM-based conditioning. Following MotionDiffuse [Zhang et al. 2024a], we enhance the features after the feed-forward network as follows:

$$\mathbf{G} = \mathbf{G} \cdot \phi_w(\phi(\mathbf{C})) + \phi_b(\phi(\mathbf{C})), \quad (12)$$

where (\cdot) denotes the element-wise product, and ϕ , ϕ_w , and ϕ_b are learnable linear projection functions. Intuitively, ϕ_w and ϕ_b act as adaptive scaling and shifting operations, respectively, allowing the motion context to modulate the gaze features dynamically.

Output projection. The output from the final Transformer block is projected through an MLP to predict the added noise estimate, which is used in the reverse diffusion process to iteratively reconstruct the imputed gaze sequence.

4.4 Gaze Generation

Gaze generation can be seen as a special case of gaze imputation, where the missing ratio reaches 100%. In this setting, no gaze observations are available, and the model must synthesise an entire gaze trajectory from auxiliary motion signals alone. By removing the observed gaze input and the corresponding conditional mask, HAGI++ naturally functions as a conditional generative model that produces realistic gaze sequences based solely on head movements and, when available, additional body-movement signals.

5 EXPERIMENTS - HEAD-ASSISTED GAZE IMPUTATION

As head-tracking sensors are readily integrated into modern mobile eye trackers, we first conducted experiments to evaluate the performance of HAGI++ on head-assisted gaze imputation.

5.1 Datasets

To assess the performance of HAGI++ across diverse real-world scenarios, we evaluated our method on three publicly available, large-scale datasets that include mobile eye-tracking and head movement recordings captured during everyday activities:

Nymeria [Ma et al. 2024] is the world’s largest in-the-wild human motion dataset, featuring over 300 hours of multimodal recordings from 264 participants engaged in everyday activities across 50 distinct indoor and outdoor environments. The dataset includes 30 Hz gaze data, head motion, wrist motion, body motion, and natural language descriptions. Due to its large scale and coverage of varied real-world settings, we used Nymeria for training and evaluation. Specifically, we selected recordings with well-calibrated personalised gaze data, SLAM poses from the eye tracker. We randomly partitioned these recordings into training (80%, 593 recordings, 145.8 hours), validation (5%, 38 recordings, 8.4 hours), and test (15%, 111 recordings, 28.7 hours) sets.

Ego-Exo4D [Grauman et al. 2024] is a large-scale multimodal dataset that provides synchronised egocentric and exocentric recordings of skilled human activities, covering activities such as cooking, football, music, dance, basketball, bicycle repair, and rock climbing. The egocentric recordings contain 30 Hz gaze data and SLAM-derived head poses from head-mounted devices. To assess the generalisability of HAGI++ across diverse indoor and outdoor activities, we used all 72 egocentric recordings (4.6 hours) with well-calibrated personalised gaze data for cross-dataset evaluation.

HOT3D [Banerjee et al. 2024] is an egocentric multimodal dataset for studying hand-object interactions in indoor environments. Similar to the other two datasets, it includes gaze data and head motion recordings. Since handling tools and interacting with objects are fundamental aspects of everyday activities, we incorporated HOT3D for cross-dataset evaluation. Our evaluation used all 111 (3.48 hours), containing well-calibrated personalised gaze data and SLAM poses.

5.2 Evaluation Settings

Baselines. We compared HAGI++ against several baseline approaches. These include widely used interpolation methods for gaze imputation as well as state-of-the-art deep learning-based time-series imputation techniques.

- **Head direction:** Given the strong correlation between head and eye movements, head direction was widely used as a proxy for gaze direction in prior work [Hu et al. 2020, 2024b; Nakashima et al. 2015; Sitzmann et al. 2018].
- **Linear interpolation and Nearest interpolation:** These two interpolation techniques are the most commonly used methods for handling missing values in eye-tracking research [Grootjen et al. 2024b; Kasneci et al. 2024].
- **iTransformer** [Liu et al. 2024]: A Transformer-based model designed for multiple time-series tasks, including time-series imputation.

- **DLinear** [Zeng et al. 2023]: A multilayer perceptron (MLP)-based method that models time-series trends using a moving average kernel and a seasonal component.
- **TimesNet** [Wu et al. 2023]: Converts 1D time-series data into 2D tensors with Fast Fourier Transformation and processes them using a CNN-based architecture. It was designed for multi-time-series tasks.
- **BRITS** [Cao et al. 2018]: A bidirectional RNN-based approach for time-series imputation.
- **CSDI** [Tashiro et al. 2021]: A diffusion-based generative model for time-series imputation, demonstrating superior performance over GAN-based [Miao et al. 2021] and VAE-based [Fortuin et al. 2020] methods in various imputation tasks.

Additionally, we compare HAGI++ with its predecessor, HAGI [Jiao et al. 2025a], to highlight the improvements introduced by the newly proposed architecture.

Input duration. We chose five seconds as the duration for all inputs, same as prior gaze-based deep learning models [Jiao et al. 2024; Lohr and Komogortsev 2022]. We clipped the gaze recordings in the Nymeria dataset into non-overlapped five-second segments according to the time stamps in the atomic motion descriptions. For the Ego-Exo4D and HOT3D datasets, we ignored the data within the very first and last second in each recording to ensure the data quality and clipped the recording into non-overlapping five-second segments. Following prior work [Lohr and Komogortsev 2022], all segments with more than 5% invalid gaze samples were discarded. To ensure the model only learns to reconstruct real gaze movements, all the remaining invalid gaze samples were excluded from the loss computation during training.

Data loss ratio. As in general time-series imputation, we masked a certain proportion of valid gaze data for evaluating imputation performance. The selected data loss ratios were informed by blink duration statistics and missing data ratios reported in prior research: Blinks occur approximately 20 times per minute, with each blink lasting between 150–450 milliseconds [Nyström et al. 2024; Stern et al. 1984]. Consequently, up to 10% missing data can be attributed solely to blinks [Nyström et al. 2025]. Additionally, prior studies have reported missing data ratios ranging from 20% to 60% [Holmqvist et al. 2012; Pernice and Nielsen 2009; Schnipke and Todd 2000]. Moreover, an empirical research shows that consecutive missing values last 1,325 milliseconds on average with the standard deviation of 4,076 milliseconds, and the majority of the missing segments are shorter than 1 second [Grootjen et al. 2024a]. Based on these findings, we evaluated HAGI++ under missing data conditions of 10%, 30%, and 50%. Furthermore, to assess HAGI++’s robustness in extreme scenarios, we also tested it with 90% missing data. Since the longest blink duration (450 ms) corresponds to approximately 10% of our five-second input window, we primarily evaluated HAGI++ on long blinks using a 10% missing ratio. Specifically, for each five-second gaze trajectory in our test sets, we randomly masked a continuous 10% segment of valid data. For 30% and 50% missing ratios, we simulated real-world data loss by ensuring that each masked segment lasted at least 150 milliseconds, corresponding to the shortest blink duration. This strategy ensured that the missing

data patterns realistically reflected natural gaze data loss. For the 90% missing ratio, we simulated an extreme case in which 90% of the sequence was continuously missing, reflecting real-world scenarios involving prolonged gaze loss as reported by [Grootjen et al. 2024a].

Evaluation metrics. We used two metrics for evaluation:

- **Mean Angular Error (MAE):** MAE is the most commonly used evaluation metric in previous gaze estimation research [Hu et al. 2020, 2024b, 2019; Zhang et al. 2015, 2017]. It measures the angular difference (in degrees) between the predicted and the ground truth gaze vectors. Specifically, we first converted the gaze direction from the unit spherical coordinate system (pitch, yaw) to a 3D Cartesian vector (x, y, z) and then computed the MAE as follows:

$$\text{MAE} = \frac{1}{J} \sum_{j=1}^J \arccos \left(\frac{g_j \cdot \hat{g}_j}{|g_j| |\hat{g}_j|} \right) \quad (13)$$

where J is the total number of missing frames, and g_j and \hat{g}_j represent the ground truth gaze vector and the predicted gaze vector, respectively.

- **Jensen–Shannon divergence (JS):** While MAE evaluates the accuracy of gaze direction reconstruction, it does not assess whether the imputed gaze movements exhibit realistic human gaze dynamics. To address this, we incorporated JS divergence, following prior work on eye movement synthesis [Jiao et al. 2024; Prasse et al. 2023, 2024]. JS divergence measures the similarity between the velocity distribution of imputed and real human gaze movements. Let P and Q be the distributions of the predicted and ground truth gaze velocities at missing frames, respectively. JS divergence is defined as:

$$\text{JS}(P||Q) = \frac{1}{2} \text{KL} \left(P \left\| \frac{1}{2} (P + Q) \right. \right) + \frac{1}{2} \text{KL} \left(Q \left\| \frac{1}{2} (P + Q) \right. \right), \quad (14)$$

where KL denotes the Kullback–Leibler (KL) divergence. JS divergence ranges between zero and one, with lower values indicating better performance.

A good gaze imputation method should achieve lower JS on the basis of lower MAE.

Implementation details. All datasets used in our experiments provide gaze data at 30 Hz, and we set the input duration to five seconds, resulting in a total sequence length of $L = 150$. For HAGI++, we set the number of transformer blocks to $N = 4$ and the number of attention heads to eight for self-attention and cross-attention mechanism. The diffusion process consisted of $T = 50$ steps, using a cosine noise schedule with a minimum noise level of $1 - \alpha_1 = 10^{-4}$ and a maximum noise level of $1 - \alpha_T = 0.5$. The training was conducted for 500 epochs with a batch size of 256, using the AdamW optimizer with an initial learning rate of 10^{-3} , which decayed to 10^{-4} at epoch 375 and further to 10^{-5} at epoch 450.

Since CSDI [Tashiro et al. 2021] is also a diffusion-based approach, we ensured a fair comparison by training CSDI with the same diffusion hyperparameters as HAGI++ using its official implementation. For other deep learning-based time-series imputation baselines, we leveraged PyPOTS [Du 2023], a popular Python toolbox that includes various time-series imputation methods [Du et al. 2024]. We

Nymeria	Data loss ratio			
	10%	30%	50%	90%
Head direction	23.32	23.43	23.44	23.44
Linear	4.96	6.88	9.68	11.54
Nearest	5.29	6.52	8.34	12.61
iTransformer [Liu et al. 2024]	8.75	11.10	16.57	24.05
DLinear [Zeng et al. 2023]	12.12	12.25	12.97	14.01
TimesNet [Wu et al. 2023]	19.53	18.59	20.32	22.91
BRITS [Cao et al. 2018]	10.25	11.98	14.06	17.58
CSDI [Tashiro et al. 2021]	4.72	5.90	7.44	10.54
HAGI	<u>3.67</u>	<u>4.55</u>	<u>5.77</u>	<u>8.53</u>
HAGI++	3.54	4.40	5.58	8.18

Table 1. Mean angular error (MAE) of gaze imputation across different methods and data loss ratios on the Nymeria [Ma et al. 2024] test set. The best results are marked in bold, and the second-best are underlined.

Nymeria	Data loss ratio			
	10%	30%	50%	90%
Head direction	0.139	0.137	0.139	0.146
Linear	0.129	0.078	0.089	0.150
Nearest	0.081	0.073	0.103	0.135
CSDI [Tashiro et al. 2021]	<u>0.044</u>	<u>0.042</u>	0.037	<u>0.030</u>
HAGI	0.042	0.040	0.035	0.017
HAGI++	0.045	<u>0.042</u>	<u>0.036</u>	0.017

Table 2. Jensen–Shannon divergence (JS) of gaze imputation across different methods and data loss ratios on the Nymeria [Ma et al. 2024] test set. The best results are marked in bold, and the second-best are underlined.

modified only the input shape while keeping the optimal hyperparameters provided for the PhysioNet2012 dataset [Silva et al. 2012] and trained all models with the same number of epochs and batch size. All deep learning-based methods were trained on the Nymeria training set, and we selected the best-performing model on the validation set for the final evaluation. For classical interpolation methods, we used the built-in functions from the SciPy library [Virtanen et al. 2020]. As a baseline head direction proxy, we filled in missing frames with $(\text{pitch}, \text{yaw}) = (0, 0)$. For generative models that do not produce deterministic outputs, we followed [Alcaraz and Strothoff 2022; Tashiro et al. 2021] and used the median of 100 generated samples for evaluation.

5.3 Gaze Imputation Results

Quantitative results. Table 1 presents the mean angular error (MAE) of gaze imputation across different methods and missing ratios for within-dataset evaluation on the Nymeria test set. As shown in the table, HAGI++ consistently outperforms all baselines across all levels of missing data, achieving improvements of 25% for long blinks (3.54° vs. 4.72°), 25% for 30% missing data (4.40°

vs. 5.90°), 25% for 50% missing data (5.58° vs. 7.44°), and 22.5% for 90% missing data (8.18° vs. 10.54°), compared with the second-best method that does not incorporate head information. Furthermore, the additional on average 3.6% improvement over HAGI across all missing ratios demonstrates that the new model architecture more effectively captures eye–head coordination. In contrast, except for CSDI, time-series imputation methods did not achieve performance comparable to traditional interpolation methods. This suggests that these time-series imputation methods cannot be directly adapted to gaze data without modification. Consequently, we excluded these methods from further evaluations (see Appendix A if interested).

Table 2 shows the Jensen–Shannon divergence (JS) of gaze imputation across different methods and data loss ratios, also on the Nymeria test set. The velocity distributions of gaze imputed by HAGI++ achieve performance on par with the previous state of the art, HAGI, across all experimental settings. This demonstrates that HAGI++ preserves the natural dynamics of human gaze while simultaneously achieving the lowest mean angular error relative to the ground truth, offering both higher accuracy and greater biological plausibility. In contrast, traditional interpolation methods perform substantially worse in replicating human-like eye movements than diffusion-based approaches.

We then conducted a cross-dataset evaluation on the Ego-Exo4D and HOT3D datasets to assess whether HAGI++ can generalise to diverse everyday settings. The results are shown in Table 3. Similar to the results on the Nymeria dataset, despite HAGI++ not being trained or fine-tuned on these datasets, it achieved the lowest MAE across all methods and missing ratios, with a minimum improvement of 13.2%, a maximum improvement of 22.0%, and an average improvement of 19.2% over the second-best method that does not utilise head information. Moreover, the additional 2.4% average improvement over HAGI across all missing ratios demonstrates that the new model architecture more effectively captures eye–head coordination. Finally, HAGI++ attained a comparable JS divergence to HAGI, indicating that its imputed gaze velocity distribution remains close to the natural human gaze dynamics. Moreover, it is worth noting that in the cross-dataset evaluation, the absolute MAE across different missing ratios did not decrease compared with the within-dataset results on the Nymeria dataset (see Table 1). This suggests that HAGI++ learns robust correlations between eye and head movements that generalise well across datasets featuring diverse everyday activities and environments, demonstrating strong generalisation performance and reflecting the benefits of training on a larger and more diverse dataset.

Qualitative results. We present four sample gaze imputation results from the cross-dataset evaluation for five methods with relatively low MAE in Figure 3. As shown in Figure 3, HAGI++ benefits from the incorporation of head movement information, producing imputed gaze trajectories that more closely follow the ground-truth human eye movements both spatially and temporally. At 30% and 50% missing ratios, HAGI++ exhibits a trajectory trend that is closer to the ground truth compared with HAGI, highlighting the effectiveness of the new architecture. Even in the challenging scenario with 90% missing values, both HAGI++ and HAGI generate gaze samples that remain well aligned with the ground truth. This suggests

Dataset	Mean angular error (MAE)								Jensen–Shannon divergence (JS)							
	Ego-Exo4D				HOT3D				Ego-Exo4D				HOT3D			
Data loss ratio	10%	30%	50%	90%	10%	30%	50%	90%	10%	30%	50%	90%	10%	30%	50%	90%
Head direction	25.82	25.76	25.88	25.82	23.63	23.81	23.70	23.73	0.126	0.125	0.124	0.131	0.148	0.148	0.147	0.145
Linear	3.92	5.54	7.90	9.29	3.87	5.64	7.80	8.98	0.094	0.085	0.073	0.135	0.277	0.102	0.096	0.148
Nearest	4.18	5.18	6.68	10.13	4.14	5.23	6.61	9.86	0.062	0.066	0.081	0.121	0.080	0.081	0.100	0.135
CSDI [Tashiro et al. 2021]	3.78	4.78	6.07	8.91	3.67	4.69	5.85	8.28	<u>0.042</u>	0.041	0.033	0.026	<u>0.052</u>	<u>0.051</u>	<u>0.042</u>	0.029
HAGI	<u>3.06</u>	<u>3.80</u>	<u>4.86</u>	<u>7.37</u>	<u>3.01</u>	<u>3.91</u>	<u>4.99</u>	<u>7.34</u>	0.040	0.041	0.033	<u>0.024</u>	0.049	0.050	0.040	0.021
HAGI++	2.98	3.73	4.76	7.08	2.94	3.84	4.86	7.19	0.044	<u>0.043</u>	<u>0.034</u>	0.023	0.055	0.053	<u>0.042</u>	<u>0.022</u>

Table 3. Cross-dataset evaluation results: Mean angular error (MAE) and Jensen–Shannon divergence (JS) of gaze imputation across different methods and data loss ratios on the Ego-Exo4D [Grauman et al. 2024] and HOT3D [Banerjee et al. 2024] datasets. The best results are marked in bold, and the second-best are underlined.

that leveraging head movements provides valuable contextual information for gaze imputation, enabling HAGI++ to generate more naturalistic and human-like gaze trajectories compared to baseline methods, aligning with results of MAE in Table 3. In contrast, the gaze trajectories imputed by traditional interpolation methods are visually dissimilar to real human eye movements. This visual assessment aligns with the JS values reported in Table 3. Although CSDI achieved a low JS score in Table 3, its imputed gaze data exhibits substantial spatial deviation from real human eye movements.

5.4 Head Rotation vs. Translation.

The evaluation results so far show that incorporating head information enables HAGI++ to achieve superior performance over single-modal baseline approaches. However, as discussed in Section 4.3, the input head movements comprise rotation and translation. It remains unclear how head rotation and head translation separately contribute to gaze imputation performance. To gain further insight into this question, we trained two ablated versions of HAGI and HAGI++, respectively: one that receives only head rotation matrices as input and another that receives only head translation vectors.

The results are shown in Table 4. Since prior work [Jiao et al. 2025b, 2024] and our previous findings demonstrated that diffusion-based approaches effectively model gaze velocity distributions, we report only the MAE in our results. Compared with CSDI, which does not utilise head information, HAGI++ trained with only head rotation achieves lower MAE across all settings and datasets, while HAGI++ trained with only head translation performs better in 10 out of 12 cases. This suggests that both head rotation and translation are correlated with human eye gaze and are both important to achieve performance improvements. Furthermore, HAGI++ rotation consistently outperforms HAGI++ translation, suggesting that head rotation contributes more to gaze imputation performance than head translation. The full HAGI++, trained with the complete head transformation matrices, outperforms both ablated versions, demonstrating its ability to leverage the full range of head motion for enhanced gaze imputation accuracy. Notably, even the rotation-only variant of HAGI++ consistently outperforms HAGI, further underscoring the benefits of the new architecture design.

5.5 Efficiency Comparison

Since CSDI, HAGI, and HAGI++ are all capable of imputing missing gaze samples at arbitrary locations within a five-second time window, one potential application is to perform real-time imputation during data collection. We compared GPU memory consumption and inference time for imputing a batch of 512 five-second gaze sequences across the three methods. All models were evaluated using the same inference script on a single NVIDIA Tesla V100 GPU (32 GB) equipped with two Intel(R) Xeon(R) Platinum 8160 CPUs and 1.5 TB of RAM. As shown in Table 5, HAGI++ substantially reduces both memory consumption and inference time compared with the baselines, while achieving the most accurate gaze prediction results.

5.6 Ablation Study

We finally conducted an ablation study to evaluate the effectiveness of the key design components in HAGI++. Table 6 reports the MAE results for the ablated variants of our model across different missing ratios on the Nymeria, Ego-Exo4D, and HOT3D datasets. The version of HAGI++ without head movements and the proposed feature-fusion mechanism consistently produced the highest MAE across all settings. Incorporating head information reduced the MAE, yielding an average improvement of 19.6% compared with the variant that used only the observed gaze for prediction. Furthermore, by introducing the proposed skip fusion based on FiLM conditioning, the full HAGI++ achieved an additional average improvement of 0.7% over the version with head information only. These findings highlight the contribution of each proposed component to the overall performance of HAGI++. Notably, the ablated version of HAGI++ using only gaze information still outperforms CSDI, and the version using only head information consistently surpasses HAGI, underscoring the strength of the proposed architectural design.

6 EXPERIMENTS – HEAD–WRIST-ASSISTED GAZE IMPUTATION

Since human hand movements are known to be correlated with eye movements [Binsted et al. 2001; Johansson et al. 2001], and hand or wrist motions can be readily captured using commercial smartwatches, wristbands, or hand controllers commonly paired with XR headsets, we further extend HAGI++ by incorporating wrist movement information as an additional input modality. This experiment

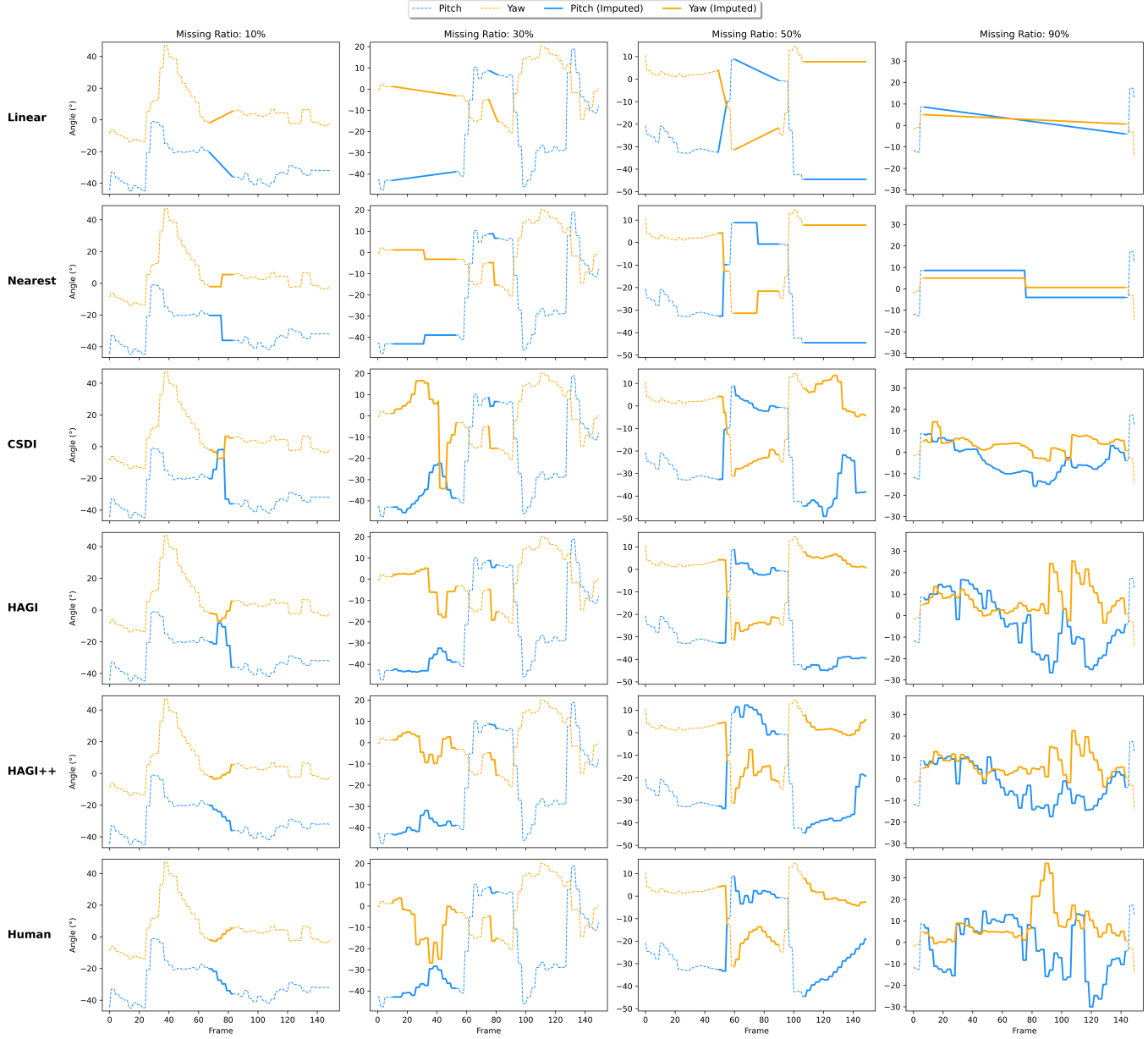


Fig. 3. Four examples of gaze imputation results at different missing ratios (10%, 30%, 50%, 90%) using different methods in the cross-dataset evaluation. The bottom row shows the visualisations of ground truth human eye movements.

investigates whether wrist movements can further enhance gaze imputation performance beyond head-assisted modelling.

6.1 Datasets

The Nymeria dataset [Ma et al. 2024] includes synchronised wrist motion data recorded using two wristbands worn on participants’ left and right wrists, making it suitable for our experiments. Specifically, we used a subset of the Nymeria dataset (145.1 hours for training, 8.3 hours for validation, and 28.7 hours for testing) derived

from the same data used in Section 5, after excluding recordings without valid wrist motion data for both wrists. Given that HAGI++, when trained on Nymeria, demonstrated strong generalisability in the head-assisted gaze imputation experiments (Section 5), and that the dataset is sufficiently large to capture diverse real-world variations, we conducted our evaluations exclusively on this dataset.

	Head movements		Nymeria				Ego-Exo4D			HOT3D				
	Rotation	Translation	10%	30%	50%	90%	10%	30%	50%	90%	10%	30%	50%	90%
CSDI [Tashiro et al. 2021]	✗	✗	4.72	5.90	7.44	10.54	3.78	4.78	6.07	8.91	3.67	4.69	5.85	8.28
HAGI	✗	✓	4.66	5.75	7.29	10.47	3.72	4.63	5.91	8.79	3.60	4.57	5.74	8.19
	✓	✗	4.41	5.36	6.66	9.56	3.55	4.35	5.43	8.23	3.42	4.33	5.38	7.79
	✓	✓	3.67	4.55	5.77	8.53	3.06	3.80	4.86	7.37	3.01	3.91	4.99	7.34
HAGI++	✗	✓	4.65	5.79	7.34	10.65	3.74	4.63	5.89	8.78	3.61	4.60	5.75	8.38
	✓	✗	<u>3.60</u>	<u>4.48</u>	<u>5.69</u>	<u>8.42</u>	<u>3.02</u>	<u>3.79</u>	<u>4.86</u>	<u>7.36</u>	<u>2.95</u>	<u>3.88</u>	<u>4.95</u>	<u>7.36</u>
	✓	✓	3.54	4.40	5.58	8.18	2.98	3.73	4.76	7.08	2.94	3.84	4.86	7.19

Table 4. The results (mean angular error) of the ablation study on head rotation and translation across different data loss ratios in the Nymeria [Ma et al. 2024], Ego-Exo4D [Grauman et al. 2024], and HOT3D [Banerjee et al. 2024] datasets. The best results are marked in bold, and the second-best are underlined.

	Memory (MB)	Inference Time (s)
CSDI [Tashiro et al. 2021]	3848	<u>4.895</u>
HAGI	4380	7.484
HAGI++	2608	3.455

Table 5. The GPU memory consumption and inference time for three methods tested on one Nvidia Tesla V100 (32GB) GPU with a batch size of 512 during inference. The best results are marked in bold, and the second-best are underlined.

6.2 Evaluation Settings

We adopted the same input duration, data loss ratios, and evaluation metrics as described in Section 5. Since the dataset used here remains largely unchanged, we compared our method only against HAGI [Jiao et al. 2025a], which achieved the second-best performance in the head-assisted gaze imputation experiments.

To evaluate performance across different real-world usage scenarios, we trained several variants of HAGI++:

- HAGI++: using only head movements as input, simulating scenarios where only head-tracking information is available.
- HAGI++ (Head + One Wrist): incorporating an additional input from a single wrist, representing setups where the user wears a mobile eye tracker and one wristband.
- HAGI++ (Head + Two Wrists): integrating both left- and right-wrist motion signals, corresponding to XR headset setups equipped with two hand controllers.

All models and baselines were trained on the dataset using identical hyperparameters as specified in Section 5.

6.3 Gaze Imputation Results

Since all compared methods are diffusion-based and inherently capable of modelling gaze velocity distributions, we report only the mean angular error (MAE) in this experiment. The results are presented in Table 7.

Moreover, incorporating wrist information further improves performance, particularly under higher missing ratios. For instance, at a 90% data loss ratio, the best result is achieved when using both wrists, yielding a 3.5% improvement over the head-only HAGI++

variant (7.88° vs. 8.17°). In contrast, when the data loss ratio is low (e.g. 10%), all variants of HAGI++ exhibit nearly identical performance. These findings suggest that over short periods of missing data (e.g. within 450 ms, corresponding to a typical blink duration), eye-head coordination plays the dominant role in guiding gaze behaviour, whereas over longer durations, eye-hand coordination begins to contribute more substantially to gaze prediction.

7 EXPERIMENTS – GAZE GENERATION

When the data loss ratio reaches 100%, the gaze imputation task becomes equivalent to *gaze generation*. As described in Section 4.4, HAGI++ can be readily adapted to this setting with only minor modifications. In addition, generating gaze purely from head and other body movements captured by commodity wearable devices offers a promising solution for XR headsets such as the Meta Quest 3 [Meta Platforms Inc. 2023], which lack built-in eye-tracking capabilities. To this end, we evaluated HAGI++ for gaze generation using the same dataset described in Section 6.

7.1 Evaluation Settings

We adopted the same input duration and evaluation metrics as those used in Sections 5 and 6, while setting the data loss ratio to 100%. Similar to Section 6, to examine performance under different real-world configurations, we trained multiple variants of HAGI++, including the head-only model (HAGI++), HAGI++ with one wrist, and HAGI++ with two wrists. All models were trained using the same hyperparameters specified in Section 5.

We compared HAGI++ with:

- **Pose2Gaze** [Hu et al. 2024b]: Utilises head orientation and full-body poses to predict gaze direction using a CNN and a graph convolutional network. It has been shown to outperform previous gaze-generation methods based solely on head motion [Hu et al. 2021, 2020]. Since the Nymeria dataset provides full-body poses, we adapted the input to use 23 joints (instead of the original 21) to match the dataset’s format. We retained the authors’ hyperparameters, trained the model for the same number of epochs and batch size as HAGI++, and selected the best-performing checkpoint based on validation performance. It is worth noting, however,

	HAGI++ components		Nymeria				Ego-Exo4D			HOT3D				
	Head information	FiLM fusion	10%	30%	50%	90%	10%	30%	50%	90%	10%	30%	50%	90%
CSDI [Tashiro et al. 2021]	✗	✗	4.72	5.90	7.44	10.54	3.78	4.78	6.07	8.91	3.67	4.69	5.85	8.28
HAGI	✓	✗	3.67	4.55	5.77	8.53	3.06	3.80	4.86	7.37	3.01	3.91	4.99	7.34
HAGI++ (Ours)	✗	✗	4.61	5.74	7.27	10.38	3.70	4.61	5.92	8.78	3.58	4.56	5.72	8.23
	✓	✗	<u>3.55</u>	<u>4.42</u>	<u>5.61</u>	<u>8.24</u>	<u>2.99</u>	<u>3.75</u>	<u>4.79</u>	<u>7.18</u>	<u>2.96</u>	<u>3.86</u>	<u>4.90</u>	<u>7.26</u>
	✓	✓	3.54	4.40	5.58	8.18	2.98	3.73	4.76	7.08	2.94	3.84	4.86	7.19

Table 6. The results (mean angular error) of the ablation study on different HAGI++ components across different data loss ratios in the Nymeria [Ma et al. 2024], Ego-Exo4D [Grauman et al. 2024], and HOT3D [Banerjee et al. 2024] datasets. The best results are marked in bold, and the second-best are underlined.

Nymeria	Data loss ratio			
	10%	30%	50%	90%
HAGI	4.01	4.94	6.34	9.17
HAGI++	<u>3.53</u>	<u>4.41</u>	5.67	8.17
HAGI++ + Left Wrist	3.52	4.34	<u>5.52</u>	<u>7.98</u>
HAGI++ + Right Wrist	3.61	4.48	5.68	8.09
HAGI++ + Two Wrists	3.54	4.34	5.49	7.88

Table 7. Mean angular error (MAE) of gaze imputation across different methods and data loss ratios on the Nymeria [Ma et al. 2024] (Wrist) test set. The best results are marked in bold, and the second-best are underlined.

Nymeria	MAE	JS
Pose2Gaze [Hu et al. 2024b]	13.09	0.238
HAGI++	11.65	<u>0.138</u>
HAGI++ + Left Wrist	11.28	0.153
HAGI++ + Right Wrist	<u>10.98</u>	0.156
HAGI++ + Two Wrists	10.79	0.064

Table 8. Mean angular error (MAE) and Jensen–Shannon divergence (JS) of gaze generation across different methods on the Nymeria [Ma et al. 2024] (Wrist) test set. The best results are marked in bold, and the second-best are underlined.

that capturing full-body poses in real-world settings remains challenging.

We did not compare against HOIGaze [Hu et al. 2025b], as it requires precise hand gestures and object interaction information in world coordinates—data that are difficult to capture using commodity wearable devices and are not available in the Nymeria dataset.

7.2 Gaze Generation Results

Quantitative results. The quantitative results are presented in Table 8. All variants of HAGI++ achieved lower MAE and JS divergence compared with previous state-of-the-art methods, indicating that the gaze generated by HAGI++ is both more accurate and closer to real human gaze behaviour in terms of velocity distribution. Among all the variants, the three-point version of HAGI++ (Head +

Two Wrists) achieved the best performance, with an MAE improvement of 17.6% (10.79 vs. 13.09) over Pose2Gaze and the lowest JS divergence of 0.064. These results suggest that by jointly leveraging eye–head–hand coordination captured from wearable devices, HAGI++ can generate more accurate and biologically plausible gaze trajectories compared with baselines that rely on full-body motion capture.

Interestingly, the two-point variants (HAGI++ + Left Wrist and HAGI++ + Right Wrist) achieved slightly lower MAE (11.28 and 10.98 vs. 11.65) compared with the head-only version, but exhibited higher JS divergence (0.153 and 0.156 vs. 0.138). This indicates that while wrist motion contributes additional spatial cues that improve accuracy, it may also introduce noise that slightly alters the velocity distribution. Overall, these findings confirm that multi-point motion signals from the head and wrists provide complementary information for generating realistic and temporally consistent gaze trajectories.

Qualitative results. Figure 4 visualises the gaze generation results of different HAGI++ variants alongside the state-of-the-art Pose2Gaze, which requires full-body pose input. All variants of our method achieve higher gaze generation accuracy while relying only on signals from commodity wearable devices. In the first three rows, the 3-point HAGI++ yields the lowest MAE, indicating that eye movements are closely correlated with wrist motions during these periods. In contrast, in the last row, the head-only HAGI++ achieves the lowest MAE, suggesting that head movements dominate the eye–head–hand coordination at that time. 50 additional randomly selected qualitative video examples for each method are provided in the supplementary materials.

7.3 Wrist Rotation vs. Translation

The evaluation results thus far demonstrate that incorporating wrist motions from both sides enables HAGI++ to achieve superior performance compared with the head-only version. However, as discussed in Section 4.1, the wrist-motion inputs comprise relative rotation and translation matrices between the wrists and the head. It remains unclear how these two motion components separately contribute to gaze generation performance. To gain further insight, we trained two ablated versions of HAGI++, respectively: one that receives only rotation matrices from both wrists as input and another that receives only translation vectors.

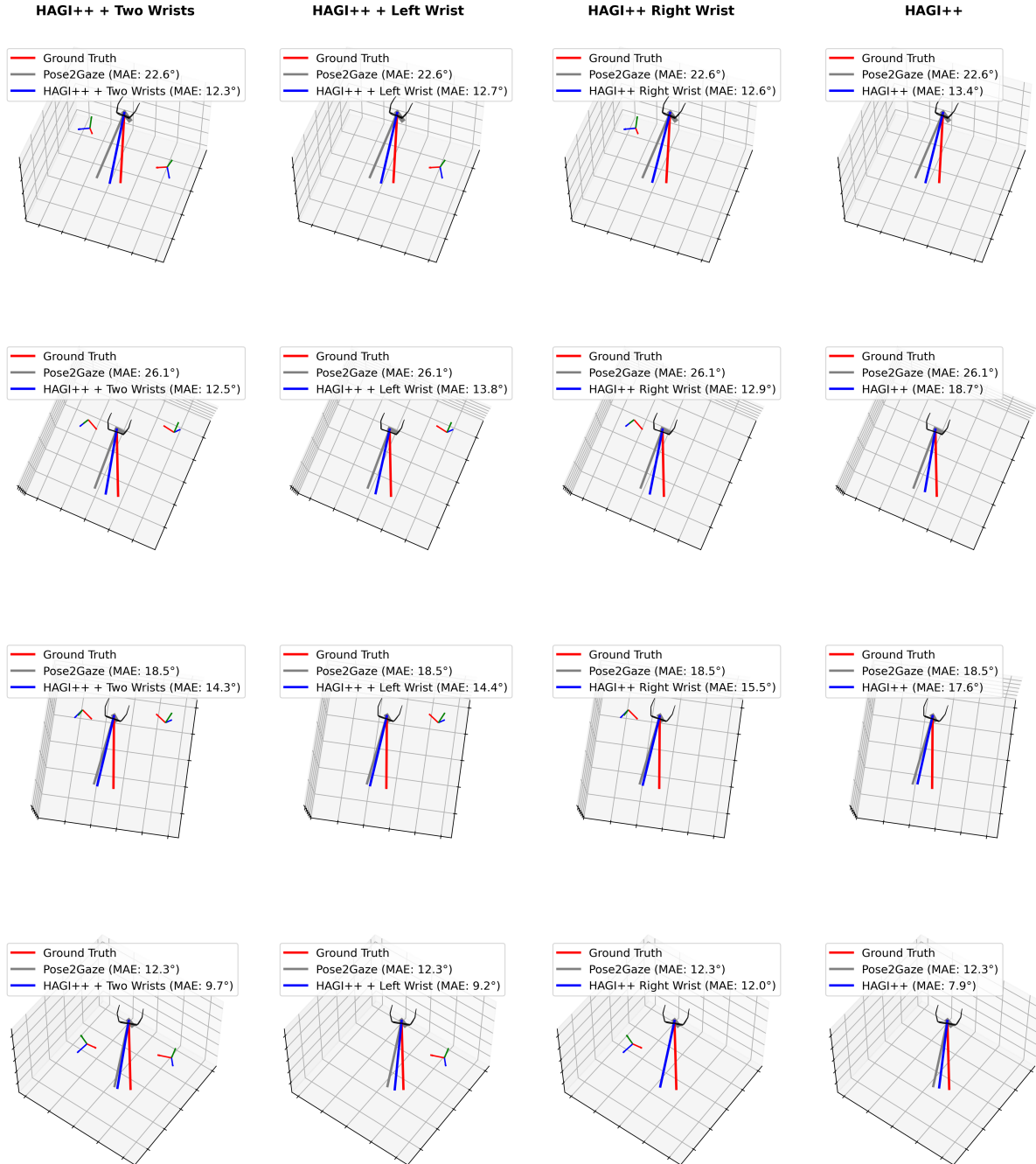


Fig. 4. Visualisation of the gaze generation results of one-point, two-point, three-point HAGI++ and the state-of-the-art method Pose2Gaze [Hu et al. 2024b] that requires full-body pose as input on the Nymeria dataset. Our method exhibits higher gaze generation accuracy with input from only commodity wearable devices. More videos can be found in our supplementary materials.

The results are presented in Table 9. Both ablated versions achieved lower MAE compared with the head-only version, indicating that wrist rotation and translation each contribute to improving gaze prediction accuracy. However, their JS divergences remained similar

to that of the head-only version. When combining rotation and translation, the model further improved gaze generation accuracy and reduced the JS divergence from 0.138, 0.129, and 0.145 to 0.064.

	Wrist movements		MAE	JS
	Rotation	Translation		
HAGI++	✗	✗	11.65	0.138
HAGI++ + Two Wrists	✗	✓	11.46	0.145
HAGI++ + Two Wrists	✓	✗	<u>11.35</u>	<u>0.129</u>
HAGI++ + Two Wrists	✓	✓	10.79	0.064

Table 9. The results (mean angular error) of the ablation study on wrist rotation and translation on the Nymeria [Ma et al. 2024] (Wrist) test set. The best results are marked in bold, and the second-best are underlined.

This suggests that wrist rotation and translation provide complementary cues jointly enabling HAGI++ to leverage eye-head-hand coordination to synthesise more accurate and natural gaze trajectories.

8 DISCUSSION

8.1 Performance

Gaze Imputation. What all of our evaluations show is that HAGI++ not only achieves superior MAE reductions but also generates gaze trajectories that more faithfully resemble natural human eye movements, highlighting its robustness and effectiveness in real-world applications. Our method consistently outperforms baseline approaches both quantitatively (see Tables 1, and 3) and qualitatively (see Figure 3) for all considered data loss ratios and datasets. In terms of mean angular error (MAE), HAGI++ reduces MAE by an average of 24.45% compared with the previous state-of-the-art method. Notably, Table 1 and Table 3 show that HAGI++’s MAE on 30% missing values is lower than MAEs of baseline methods on only 10% missing data, and its MAE on 50% missing values is similar to the MAEs of baseline methods on 30% data loss. This suggests that in real-world scenarios, HAGI++ can impute gaze data with an additional 20% missing values while maintaining/outperforming existing methods’ performance level. Importantly, as shown in Table 5, HAGI++ is also more efficient at inference time, requiring less GPU memory and achieving faster inference speed, making it highly suitable for real-world applications. This finding is significant as it shows not only the effectiveness of our method on benchmarks but also the concrete benefits it provides for practical mobile eye-tracking applications.

Unlike MAE, which tends to increase with higher levels of missing data, the Jensen-Shannon (JS) divergence of HAGI++ *decreases* as the missing ratio increases. We compute gaze velocity distributions using the `numpy.histogram` function with `bins=100` across all settings. However, the resulting absolute JS values are not directly comparable across missing ratios or datasets. For example, at 90% missingness, the ground-truth velocity distribution is considerably broader than that at 10%, with the latter effectively forming a subset of the former. Applying the same number of bins to both leads to differing bin widths, which in turn affects the scale of JS divergence. This makes direct cross-ratio or cross-dataset comparisons of JS scores inappropriate. Nonetheless, within each dataset and missing ratio, comparisons across methods remain valid. HAGI++ on par JS divergence with the state-of-the-art, indicating that it generates gaze trajectories with plausible velocity distributions.

As shown in Table 1, existing time-series imputation models that are not based on diffusion perform worse than even standard interpolation techniques when applied to gaze data. This supports prior findings [Jiao et al. 2025b] that diffusion models are better suited to modelling gaze velocity distributions. Non-diffusion methods often overfit to slow eye movements, such as fixations, which dominate real-world gaze recordings. While augmenting non-diffusion base-lines with head movement information is technically feasible, it is unlikely to yield significant improvements, as the underlying distribution of gaze velocities remains unchanged. We therefore focus on diffusion-based approaches and demonstrate that integrating head input within this framework yields further improvements in performance.

Gaze Generation. HAGI++ can also be adapted for gaze generation. The results presented in Section 7.2 demonstrate that even when relying solely on signals from wearable devices, all variants of HAGI++ outperform prior state-of-the-art gaze prediction methods that depend on full-body motion capture, achieving improvements ranging from 11.0% (HAGI++ with head only) to 17.6% (3-point HAGI++) in MAE and lower JS divergence scores. This indicates that HAGI++ can effectively synthesise more accurate and biologically plausible gaze trajectories using only head and wrist movements—signals that can be readily captured by off-the-shelf wearable devices such as XR headsets and smartwatches—making it a practical and accessible solution for gaze generation in everyday contexts.

8.2 Head Rotation vs. Translation

To investigate the independent contributions of head rotation and head translation to gaze imputation, we conducted an ablation study. The results indicate that gaze imputation benefits from head rotation and translation; however, head rotation exhibits a stronger correlation with human gaze than head translation (Table 4). This finding aligns well with prior research on vestibular function testing. In particular, dynamic visual acuity (DVA) is primarily governed by the vestibulo-ocular reflex (VOR), which stabilises gaze during head movements [Ramaoli et al. 2019]. Ramaoli et al. [Ramaoli et al. 2019] demonstrated that DVA is consistently lower during head translations (tVOR) than during head rotations (rVOR), further supporting our conclusion that head rotation plays a more dominant role in eye-head coordination.

8.3 Eye–Hand–Head Coordination

As shown in Table 7, incorporating additional wrist information does not lead to a notable improvement in MAE at low data loss ratios (e.g., 10% and 30%), where the performance remains comparable to the head-only version of HAGI++. This suggests that over short time windows, eye movements are more strongly coupled with head movements, while hand movements contribute minimally to gaze imputation. However, as the duration of missing data increases, head and hand movements begin to play a more substantial role, as evidenced by the improvements observed in the 90% and 100% missing data cases (Tables 7 and 8). In particular, under the 100% missing condition, incorporating motion signals from both wrists enhances performance in terms of both MAE and JS divergence compared with the head-only version. Furthermore, our ablation

study shows that wrist rotation and translation each contribute to performance gains, complementing one another in capturing the underlying eye–hand–head coordination. These findings collectively highlight the synergistic relationship between eye, head, and hand movements, which HAGI++ effectively exploits to infer more accurate and natural gaze behaviour.

8.4 Generalisability and Application

As demonstrated in Section 5.3, HAGI++’s performance remained consistent in cross-dataset evaluations, showing no degradation in MAE compared to within-dataset evaluations. This suggests that HAGI++ can be directly applied in real-world scenarios without requiring retraining or fine-tuning, provided that the SLAM poses of the mobile eye tracker are available. Furthermore, our results indicate that even when using only head rotation, HAGI++ still outperforms existing approaches. This highlights its adaptability; for mobile eye trackers lacking a SLAM system, HAGI++ can utilise rotation data from IMUs to achieve robust gaze imputation. While our task definition assumes perfect time alignment between head and eye movements, the real-world dataset used in our experiments includes a natural temporal offset of approximately 0–50 milliseconds. The strong performance of HAGI++ under these conditions suggests that it is resilient to small delays between head and gaze signals, further supporting its practicality in real-world use.

HAGI++ can be employed in three primary ways. First, it can be a post-processing method, particularly beneficial for preparing gaze data for machine learning models. Since machine learning approaches cannot handle missing values directly, HAGI++ can impute these values in a human-like manner, enhancing data utilisation efficiency. Second, HAGI++ can be used to synthesise eye-tracking data for headsets that lack built-in eye-tracking functionality, leveraging signals from embedded sensors or off-the-shelf wearable devices. This capability can also benefit digital human or character animation by reducing the need for labour-intensive eye motion capture. Third, a key advantage of HAGI++ is its ability to impute gaze data at arbitrary locations within a 5-second time window. This means that after an initial 5-second recording period, any newly encountered missing values can be imputed directly with HAGI++. This capability makes HAGI++ promising for gaze-based interactive systems. However, as shown in Table 5, the current inference—remains a limitation for real-time deployment. We plan to optimise the model’s efficiency to support real-time gaze interaction, such as gaze-based selection, foveated rendering, or attention-aware interfaces, in future work.

8.5 Limitations and Future Work

HAGI++ is designed for gaze imputation in mobile eye tracking scenarios, and all evaluations in this work were conducted on egocentric datasets involving everyday human activities. While this setting reflects realistic use cases for head-mounted eye trackers, advanced stationary eye trackers—such as the Tobii Eye Tracker 5 [Tobii AB 2023]—also support head tracking and may benefit from our approach. In future work, we aim to investigate the adaptability of HAGI++ to such desktop setups.

While our quantitative and distributional results demonstrate that HAGI++ produces realistic gaze trajectories at 30 Hz, we have

not evaluated its performance on higher-frequency gaze data. As modern mobile eye trackers typically provide head-tracking sensors at higher sampling rates, head features can, in principle, support higher-frequency gaze imputation. However, this would require retraining the model, and current public datasets with high-frequency gaze recordings are limited. We aim to investigate this direction in future work.

Additionally, although our task assumes synchronised head and eye data, our experiments used datasets where head and gaze signals have an inherent delay of around 0–50 ms. This suggests that HAGI++ is robust to small misalignments. In future work, we intend to assess its tolerance to longer delays, which are common in practice due to imperfect sensor synchronisation.

Finally, in this work we only utilise motion data captured by wearable devices. However, modern mobile eye trackers and XR headsets also provide egocentric video recordings, and human gaze is strongly influenced by visual stimuli. We plan to incorporate egocentric video information into HAGI++ to jointly model visual context and body motion in future work.

9 CONCLUSION

In this work, we introduced HAGI++—a novel multi-modal diffusion-based approach for gaze data imputation that leverages eye–head coordination to reconstruct missing gaze samples in a biologically plausible manner. We conducted comprehensive evaluations on three large-scale egocentric datasets—Nymeria, Ego-Exo4D, and HOT3D—and demonstrated that HAGI++ consistently outperforms both conventional interpolation and state-of-the-art deep learning baselines. Specifically, HAGI++ achieves up to a 25.3% improvement in mean angular error and produces gaze velocity distributions that more closely resemble natural human eye movements. Furthermore, by incorporating wrist motion captured from off-the-shelf wearable devices, HAGI++ extends seamlessly to gaze generation and surpasses existing full-body motion-based methods. Overall, our findings underscore the value of modelling multi-modal eye–head–hand coordination for gaze synthesis and highlight HAGI++ as a robust and practical solution for enhancing gaze data quality in real-world and XR environments.

ACKNOWLEDGMENTS

This project has received funding from the European Union’s Horizon Europe research and innovation funding programme under grant agreement No. 101072410.



Funded by
the European Union

REFERENCES

- Yasmeen Abdrabou, Yomna Abdelrahman, Mohamed Khamis, and Florian Alt. 2021. Think harder! Investigating the effect of password strength on cognitive load during password creation. In *Extended Abstracts of the 2021 CHI Conference on Human Factors in Computing Systems*. 1–7.
- Juan Lopez Alcaraz and Nils Strodthoff. 2022. Diffusion-based Time Series Imputation and Forecasting with Structured State Space Models. *Transactions on Machine Learning Research* (2022). <https://openreview.net/forum?id=hHilbk7ApW>

- Tobias Appel, Natalia Sevchenko, Franz Wortha, Katerina Tsarava, Korbinian Moeller, Manuel Ninaus, Enkelejda Kasneci, and Peter Gerjets. 2019. Predicting cognitive load in an emergency simulation based on behavioral and physiological measures. In *2019 International Conference on Multimodal Interaction*. 154–163.
- Apple Inc. 2023. *Apple Vision Pro*. Mixed Reality Headset. Available at: <https://www.apple.com/apple-vision-pro/> (Accessed on: 21 March 2025).
- Claudio Aracena, Sebastián Basterrech, Václav Snáel, and Juan Velásquez. 2015. Neural networks for emotion recognition based on eye tracking data. In *2015 IEEE International Conference on Systems, Man, and Cybernetics*. IEEE, 2632–2637.
- Mohammed Safayet Arefin, J Edward Swan II, Russell A Cohen Haffing, and Steven M Thurman. 2022. Estimating perceptual depth changes with eye vergence and inter-pupillary distance using an eye tracker in virtual reality. In *2022 Symposium on Eye Tracking Research and Applications*. 1–7.
- Jimmy Lei Ba, Jamie Ryan Kiros, and Geoffrey E Hinton. 2016. Layer normalization. *arXiv preprint arXiv:1607.06450* (2016).
- Prithviraj Banerjee, Sindi Shkodrani, Pierre Moulon, Shreyas Hampali, Shangchen Han, Fan Zhang, Linguang Zhang, Jade Fountain, Edward Miller, Selen Basol, Richard Newcombe, Robert Wang, Jakob Julian Engel, and Tomas Hodan. 2024. HOT3D: Hand and Object Tracking in 3D from Egocentric Multi-View Videos. *arXiv preprint arXiv:2411.19167* (2024).
- Esubalew Bekele, Zhi Zheng, Amy Swanson, Julie Crittendon, Zachary Warren, and Nilanjan Sarkar. 2013. Understanding how adolescents with autism respond to facial expressions in virtual reality environments. *IEEE transactions on visualization and computer graphics* 19, 4 (2013), 711–720.
- Jennifer K Bertrand and Craig S Chapman. 2023. Dynamics of eye-hand coordination are flexibly preserved in eye-cursor coordination during an online, digital, object interaction task. In *Proceedings of the 2023 CHI conference on human factors in computing systems*. 1–13.
- Gordon Binsted, Romeo Chua, Werner Helsen, and Digby Elliott. 2001. Eye-hand coordination in goal-directed aiming. *Human movement science* 20, 4-5 (2001), 563–585.
- Pieter Blignaut and Daniël Wium. 2014. Eye-tracking data quality as affected by ethnicity and experimental design. *Behavior research methods* 46 (2014), 67–80.
- Andreas Bulling, Daniel Roggen, and Gerhard Tröster. 2008. It's in your eyes: Towards context-awareness and mobile HCI using wearable EOG goggles. In *Proceedings of the 10th international conference on Ubiquitous computing*. 84–93.
- Wei Cao, Dong Wang, Jian Li, Hao Zhou, Lei Li, and Yitan Li. 2018. Brits: Bidirectional recurrent imputation for time series. *Advances in neural information processing systems* 31 (2018).
- Wenjie Du. 2023. PyPOTS: a Python toolbox for data mining on Partially-Observed Time Series. *arXiv preprint arXiv:2305.18811* (2023).
- Wenjie Du, Jun Wang, Linglong Qian, Yiyuan Yang, Fanxing Liu, Zepu Wang, Zina Ibrahim, Haoxin Liu, Zhiyuan Zhao, Yingjie Zhou, Wenjia Wang, Kaize Ding, Yuxuan Liang, B. Aditya Prakash, and Qingsong Wen. 2024. TSI-Bench: Benchmarking Time Series Imputation. *arXiv preprint arXiv:2406.12747* (2024).
- Kara J Emery, Marina Zannoli, James Warren, Lei Xiao, and Sachin S Talathi. 2021. OpenNEEDS: A dataset of gaze, head, hand, and scene signals during exploration in open-ended vr environments. In *Proceedings of the 2021 ACM Symposium on Eye Tracking Research and Applications*. 1–7.
- Jakob Engel, Kiran Somasundaram, Michael Goesele, Albert Sun, Alexander Gamino, Andrew Turner, Arjang Talattof, Arnie Yuan, Bilal Souti, Brighid Meredith, et al. 2023. Project aria: A new tool for egocentric multi-modal ai research. *arXiv preprint arXiv:2308.13561* (2023).
- Yu Fang, Ryoichi Nakashima, Kazumichi Matsumiya, Ichiro Kuriki, and Satoshi Shioiri. 2015. Eye-head coordination for visual cognitive processing. *PLoS One* 10, 3 (2015), e0121035.
- Vincent Fortuin, Dmitry Baranchuk, Gunnar Rätsch, and Stephan Mandt. 2020. Gp-vae: Deep probabilistic time series imputation. In *International conference on artificial intelligence and statistics*. PMLR, 1651–1661.
- Jonathan Gandrud and Victoria Interrante. 2016. Predicting destination using head orientation and gaze direction during locomotion in vr. In *Proceedings of the 2016 ACM Symposium on Applied Perception*. 31–38.
- Kristen Grauman, Andrew Westbury, Lorenzo Torresani, Kris Kitani, Jitendra Malik, Triantafyllos Afouras, Kumar Ashutosh, Vijay Baiyya, Siddhant Bansal, Bikram Boote, et al. 2024. Ego-exo4d: Understanding skilled human activity from first- and third-person perspectives. In *Proceedings of the IEEE/CVF Conference on Computer Vision and Pattern Recognition*. 19383–19400.
- Jesse W Grootjen, Henrike Weingärtner, and Sven Mayer. 2023. Highlighting the Challenges of Blinks in Eye Tracking for Interactive Systems. In *Proceedings of the 2023 Symposium on Eye Tracking Research and Applications*. 1–7.
- Jesse W Grootjen, Henrike Weingärtner, and Sven Mayer. 2024a. Investigating the Effects of Eye-Tracking Interpolation Methods on Model Performance of LSTM. In *Proceedings of the 2024 Symposium on Eye Tracking Research and Applications*. 1–6.
- Jesse W Grootjen, Henrike Weingärtner, and Sven Mayer. 2024b. Uncovering and Addressing Blink-Related Challenges in Using Eye Tracking for Interactive Systems. In *Proceedings of the 2024 CHI Conference on Human Factors in Computing Systems*. 1–23.
- Nishan Gunawardena, Michael Matscheko, Bernhard Anzengruber, Alois Ferscha, Martin Schobesberger, Andreas Shamiyeh, Bettina Klugsberger, and Peter Solleder. 2019. Assessing surgeons' skill level in laparoscopic cholecystectomy using eye metrics. In *Proceedings of the 11th ACM Symposium on Eye Tracking Research & Applications*. 1–8.
- Kaiming He, Xiangyu Zhang, Shaoqing Ren, and Jian Sun. 2016. Deep residual learning for image recognition. In *Proceedings of the IEEE conference on computer vision and pattern recognition*. 770–778.
- Jonathan Ho, Ajay Jain, and Pieter Abbeel. 2020. Denoising diffusion probabilistic models. *Advances in neural information processing systems* 33 (2020), 6840–6851.
- Kenneth Holmqvist, Marcus Nyström, and Fiona Mulvey. 2012. Eye tracker data quality: What it is and how to measure it. In *Proceedings of the symposium on eye tracking research and applications*. 45–52.
- Jinghui Hu, John J Dudley, and Per Ola Kristensson. 2025a. Seeing and Touching the Air: Unraveling Eye-Hand Coordination in Mid-Air Gesture Typing for Mixed Reality. In *Proceedings of the 2025 CHI Conference on Human Factors in Computing Systems*. 1–15.
- Zhiming Hu, Andreas Bulling, Sheng Li, and Guoping Wang. 2021. FixationNet: Forecasting Eye Fixations in Task-Oriented Virtual Environments. *IEEE Transactions on Visualization and Computer Graphics (TVCG)* 27, 5 (2021), 2681–2690. <https://doi.org/10.1109/TVCG.2021.3067779>
- Zhiming Hu, Andreas Bulling, Sheng Li, and Guoping Wang. 2023. EHTask: Recognizing User Tasks From Eye and Head Movements in Immersive Virtual Reality. *IEEE Transactions on Visualization and Computer Graphics* 29, 4 (2023), 1992–2004. <https://doi.org/10.1109/TVCG.2021.3138902>
- Zhiming Hu, Daniel Haeufle, Syn Schmitt, and Andreas Bulling. 2025b. HOIGaze: Gaze Estimation During Hand-Object Interactions in Extended Reality Exploiting Eye-Hand-Head Coordination. In *Proceedings of the 2025 ACM Special Interest Group on Computer Graphics and Interactive Techniques*.
- Zhiming Hu, Sheng Li, Congyi Zhang, Kangrui Yi, Guoping Wang, and Dinesh Manocha. 2020. DGaze: CNN-based gaze prediction in dynamic scenes. *IEEE Transactions on Visualization and Computer Graphics* 26, 5 (2020), 1902–1911.
- Zhiming Hu, Syn Schmitt, Daniel Haeufle, and Andreas Bulling. 2024a. GazeMotion: Gaze-guided Human Motion Forecasting. In *Proceedings of the 2024 IEEE/RSJ International Conference on Intelligent Robots and Systems*.
- Zhiming Hu, Jiahui Xu, Syn Schmitt, and Andreas Bulling. 2024b. Pose2Gaze: Eye-body Coordination during Daily Activities for Gaze Prediction from Full-body Poses. *IEEE Transactions on Visualization and Computer Graphics* (2024).
- Zhiming Hu, Zheming Yin, Daniel Haeufle, Syn Schmitt, and Andreas Bulling. 2024c. HOIMotion: Forecasting Human Motion During Human-Object Interactions Using Egocentric 3D Object Bounding Boxes. *IEEE Transactions on Visualization and Computer Graphics* (2024).
- Zhiming Hu, Congyi Zhang, Sheng Li, Guoping Wang, and Dinesh Manocha. 2019. SGaze: a data-driven eye-head coordination model for realtime gaze prediction. *IEEE Transactions on Visualization and Computer Graphics* 25, 5 (2019), 2002–2010.
- Zhiming Hu, Guanhua Zhang, Zheming Yin, Daniel Haeufle, Syn Schmitt, and Andreas Bulling. 2025c. HaHeAE: Learning Generalisable Joint Representations of Human Hand and Head Movements in Extended Reality. *IEEE Transactions on Visualization and Computer Graphics* (2025).
- Michael Xuelin Huang and Andreas Bulling. 2019. SacCalib: reducing calibration distortion for stationary eye trackers using saccadic eye movements. In *Proceedings of the 11th ACM Symposium on Eye Tracking Research & Applications*. 1–10.
- Ryo Ishii, Yukiko I Nakano, and Toyoaki Nishida. 2013. Gaze awareness in conversational agents: Estimating a user's conversational engagement from eye gaze. *ACM Transactions on Interactive Intelligent Systems (TiIS)* 3, 2 (2013), 1–25.
- Chuhan Jiao, Zhiming Hu, Mihai Băce, and Andreas Bulling. 2023. SUPREYES: SUPER Resolution for EYES Using Implicit Neural Representation Learning. In *Proc. ACM Symposium on User Interface Software and Technology (UIST)*. 1–13. <https://doi.org/10.1145/3586183.3606780>
- Chuhan Jiao, Zhiming Hu, and Andreas Bulling. 2025a. HAGI: Head-Assisted Gaze Imputation for Mobile Eye Trackers. In *Proc. ACM Symposium on User Interface Software and Technology (UIST)*. 1–14. <https://doi.org/10.1145/3586183.3606780>
- Chuhan Jiao, Yao Wang, Guanhua Zhang, Mihai Băce, Zhiming Hu, and Andreas Bulling. 2025b. DiffGaze: A Diffusion Model for Modelling Fine-grained Human Gaze Behaviour on 360° Images. *ACM Trans. Interact. Intell. Syst.* (Oct. 2025). <https://doi.org/10.1145/3772075>
- Chuhan Jiao, Guanhua Zhang, Zhiming Hu, and Andreas Bulling. 2024. DiffEyeSyn: Diffusion-based User-specific Eye Movement Synthesis. *arXiv preprint arXiv:2409.01240* (2024).
- Roland S Johansson, Göran Westling, Anders Bäckström, and J Randall Flanagan. 2001. Eye-hand coordination in object manipulation. *Journal of neuroscience* 21, 17 (2001), 6917–6932.
- Enkelejda Kasneci, Hong Gao, Suleyman Ozdel, Virmarie Maquiling, Enkeleida Thaqi, Carrie Lau, Yao Rong, Gjergji Kasneci, and Efe Bozkir. 2024. Introduction to Eye Tracking: A Hands-On Tutorial for Students and Practitioners. *arXiv preprint*

- arXiv:2404.15435 (2024).
- Peter Kiefer, Ioannis Giannopoulos, Martin Raubal, and Andrew Duchowski. 2017. Eye tracking for spatial research: Cognition, computation, challenges. *Spatial Cognition & Computation* 17, 1-2 (2017), 1–19.
- Zhifeng Kong, Wei Ping, Jiayi Huang, Kexin Zhao, and Bryan Catanzaro. 2021. DiffWave: A Versatile Diffusion Model for Audio Synthesis. In *International Conference on Learning Representations*. <https://openreview.net/forum?id=a-xFK8Ymz5J>
- Rakshit Kothari, Zhizhuo Yang, Christopher Kanan, Reynold Bailey, Jeff B Pelz, and Gabriel J Diaz. 2020. Gaze-in-wild: A dataset for studying eye and head coordination in everyday activities. *Scientific Reports* 10, 1 (2020), 2539.
- Tiffany CK Kwok, Peter Kiefer, Victor R Schinazi, Benjamin Adams, and Martin Raubal. 2019. Gaze-guided narratives: Adapting audio guide content to gaze in virtual and real environments. In *Proceedings of the 2019 CHI Conference on Human Factors in Computing Systems*. 1–12.
- Mikko Kytö, Barrett Ens, Thammathip Piumsomboon, Gun A Lee, and Mark Billinghurst. 2018. Pinpointing: precise head-and eye-based target selection for augmented reality. In *Proceedings of the 2018 CHI Conference on Human Factors in Computing Systems*. 1–14.
- Michael Land, Neil Mennie, and Jennifer Rusted. 1999. The roles of vision and eye movements in the control of activities of daily living. *Perception* 28, 11 (1999), 1311–1328.
- Beibin Li, Erin Barney, Caitlin Hudac, Nicholas Nuechterlein, Pamela Ventola, Linda Shapiro, and Frederick Shic. 2020. Selection of eye-tracking stimuli for prediction by sparsely grouped input variables for neural networks: towards biomarker refinement for autism. In *ACM Symposium on Eye Tracking Research and Applications*. 1–8.
- Yong Liu, Tengge Hu, Haoran Zhang, Haixu Wu, Shiyu Wang, Lintao Ma, and Mingsheng Long. 2024. iTransformer: Inverted Transformers Are Effective for Time Series Forecasting. In *The Twelfth International Conference on Learning Representations*. <https://openreview.net/forum?id=JePFAI8fah>
- Dillon Lohr and Oleg V. Komogortsev. 2022. Eye Know You Too: Toward Viable End-to-End Eye Movement Biometrics for User Authentication. *IEEE Transactions on Information Forensics and Security* 17 (2022), 3151–3164. <https://doi.org/10.1109/TIFS.2022.3201369>
- Paula López, Ana María Bernardos, and José Ramón Casar. 2024. Eye-Tracking Analysis for Cognitive Load Estimation in Wearable Mixed Reality. In *Proceedings of the 2024 ACM Symposium on Spatial User Interaction*. 1–2.
- Mathias N Lystbæk, Thorbjørn Mikkelsen, Roland Krisztandl, Eric J Gonzalez, Mar Gonzalez-Franco, Hans Gellersen, and Ken Pfeuffer. 2024. Hands-on, Hands-off: Gaze-Assisted Bimanual 3D Interaction. In *Proceedings of the 37th Annual ACM Symposium on User Interface Software and Technology*. 1–12.
- Mathias N Lystbæk, Ken Pfeuffer, Jens Emil Sloth Grønbaek, and Hans Gellersen. 2022. Exploring gaze for assisting freehand selection-based text entry in ar. *Proceedings of the ACM on Human-Computer Interaction* 6, ETRA (2022), 1–16.
- Lingni Ma, Yuting Ye, Fangzhou Hong, Vladimir Guzov, Yifeng Jiang, Rowan Postyeni, Luis Pesqueira, Alexander Gamino, Vijay Baiyya, Hyo Jin Kim, et al. 2024. Nymeria: A massive collection of multimodal egocentric daily motion in the wild. In *European Conference on Computer Vision*. Springer, 445–465.
- Pujitha Mannaru, Balakumar Balasingam, Krishna Pattipati, Ciara Sibley, and Joseph T Coyne. 2017. Performance evaluation of the gaze-point GP3 eye tracking device based on pupil dilation. In *Augmented Cognition. Neurocognition and Machine Learning: 11th International Conference, AC 2017, Held as Part of HCI International 2017, Vancouver, BC, Canada, July 9-14, 2017, Proceedings, Part 1*. Springer, 166–175.
- Meta Platforms Inc. 2022. *Meta Quest Pro*. Virtual Reality Headset. Available at: <https://www.meta.com/quest/quest-pro/> (Accessed on: 21 March 2025).
- Meta Platforms Inc. 2023. *Meta Quest 3*. Virtual Reality Headset. Available at: <https://www.meta.com/quest/quest-3/> (Accessed on: 21 March 2025).
- Xiaoye Miao, Yangyang Wu, Jun Wang, Yunjun Gao, Xudong Mao, and Jianwei Yin. 2021. Generative semi-supervised learning for multivariate time series imputation. In *Proceedings of the AAAI conference on artificial intelligence*, Vol. 35. 8983–8991.
- Microsoft Corporation. 2019. *Microsoft HoloLens 2*. Augmented Reality Headset. Available at: <https://www.microsoft.com/hololens> (Accessed on: 21 March 2025).
- Philipp Müller, Daniel Buschek, Michael Xuelin Huang, and Andreas Bulling. 2019. Reducing calibration drift in mobile eye trackers by exploiting mobile phone usage. In *Proceedings of the 11th ACM Symposium on Eye Tracking Research & Applications*. 1–9.
- Yukiko I Nakano and Ryo Ishii. 2010. Estimating user’s engagement from eye-gaze behaviors in human-agent conversations. In *Proceedings of the 15th international conference on intelligent user interfaces*, 139–148.
- Ryoichi Nakashima, Yu Fang, Yasuhiro Hatori, Akinori Hiratani, Kazumichi Matsumiya, Ichiro Kuriki, and Satoshi Shioiri. 2015. Saliency-based gaze prediction based on head direction. *Vision research* 117 (2015), 59–66.
- Marcus Nyström, Richard Andersson, Kenneth Holmqvist, and Joost Van De Weijer. 2013. The influence of calibration method and eye physiology on eyetracking data quality. *Behavior research methods* 45 (2013), 272–288.
- Marcus Nyström, Richard Andersson, Diederick C Niehorster, Roy S Hessels, and Ignace TC Hooge. 2024. What is a blink? Classifying and characterizing blinks in eye openness signals. *Behavior research methods* 56, 4 (2024), 3280–3299.
- Marcus Nyström, Ignace TC Hooge, Roy S Hessels, Richard Andersson, Dan Witzner Hansen, Roger Johansson, and Diederick C Niehorster. 2025. The fundamentals of eye tracking part 3: How to choose an eye tracker. *Behavior Research Methods* 57, 2 (2025), 67.
- Ethan Perez, Florian Strub, Harm De Vries, Vincent Dumoulin, and Aaron Courville. 2018. F1: Visual reasoning with a general conditioning layer. In *Proceedings of the AAAI conference on artificial intelligence*, Vol. 32.
- Kara Pernice and Jakob Nielsen. 2009. How to Conduct and Evaluate Usability Studies Using Eyetracking. *Nielsen Norman Group: Fremont, CA, USA* (2009).
- Paul Prasse, David Robert Reich, Silvia Makowski, Seoyoung Ahn, Tobias Scheffer, and Lena A Jäger. 2023. Sp-eyegan: Generating synthetic eye movement data with generative adversarial networks. In *Proceedings of the 2023 symposium on eye tracking research and applications*. 1–9.
- Paul Prasse, David R Reich, Silvia Makowski, Tobias Scheffer, and Lena A Jäger. 2024. Improving cognitive-state analysis from eye gaze with synthetic eye-movement data. *Computers & Graphics* 119 (2024), 103901.
- Zhehan Qu, Ryleigh Byrne, and Maria Gorlatova. 2024. “Looking” into Attention Patterns in Extended Reality: An Eye Tracking-Based Study. In *2024 IEEE International Symposium on Mixed and Augmented Reality (ISMAR)*. IEEE, 855–864.
- Cecilia Ramaioli, Luigi F Cuturi, Stefano Ramat, Nadine Lehnen, and Paul R MacNeilage. 2019. Vestibulo-ocular responses and dynamic visual acuity during horizontal rotation and translation. *Frontiers in neurology* 10 (2019), 321.
- Yunlei Ren, Yan Zhang, Zhitao Liu, and Ning Xie. 2024. Eye-hand typing: Eye gaze assisted finger typing via bayesian processes in ar. *IEEE Transactions on Visualization and Computer Graphics* 30, 5 (2024), 2496–2506.
- Susan K Schnipke and Marc W Todd. 2000. Trials and tribulations of using an eye-tracking system. In *CHI’00 extended abstracts on Human factors in computing systems*. 273–274.
- Lei Shi, Paul-Christian Bürkner, and Andreas Bulling. 2025. ActionDiffusion: An Action-aware Diffusion Model for Procedure Planning in Instructional Videos. In *Proc. IEEE/CVF Winter Conference on Applications of Computer Vision (WACV)*.
- Ludwig Sidenmark and Hans Gellersen. 2019a. Eye, head and torso coordination during gaze shifts in virtual reality. *ACM Transactions on Computer-Human Interaction* 27, 1 (2019), 1–40.
- Ludwig Sidenmark and Hans Gellersen. 2019b. Eye&Head: Synergetic Eye and Head Movement for Gaze Pointing and Selection. In *Proceedings of the 2019 ACM Symposium on User Interface Software and Technology*. 1161–1174.
- Ludwig Sidenmark, Diako Mardanbegi, Argenis Ramirez Gomez, Christopher Clarke, and Hans Gellersen. 2020. BimodalGaze: Seamlessly Refined Pointing with Gaze and Filtered Gestural Head Movement. In *Proceedings of the 2020 ACM Symposium on Eye Tracking Research and Applications*. 1–9.
- Ikaro Silva, George Moody, Daniel J Scott, Leo A Celi, and Roger G Mark. 2012. Predicting in-hospital mortality of icu patients: The physionet/computing in cardiology challenge 2012. *Computing in cardiology* 39 (2012), 245.
- Vincent Sitzmann, Ana Serrano, Amy Pavel, Maneesh Agrawala, Diego Gutierrez, Belen Masia, and Gordon Wetzstein. 2018. Saliency in VR: How do people explore virtual environments? *IEEE transactions on visualization and computer graphics* 24, 4 (2018), 1633–1642.
- John S Stahl. 1999. Amplitude of human head movements associated with horizontal saccades. *Experimental Brain Research* 126, 1 (1999), 41–54.
- Julian Steil and Andreas Bulling. 2015. Discovery of Everyday Human Activities From Long-term Visual Behaviour Using Topic Models. In *Proc. ACM International Joint Conference on Pervasive and Ubiquitous Computing (UbiComp)*. 75–85. <https://doi.org/10.1145/2750858.2807520>
- John A Stern, Larry C Walrath, and Robert Goldstein. 1984. The endogenous eyeblink. *Psychophysiology* 21, 1 (1984), 22–33.
- Yusuke Tashiro, Jiaming Song, Yang Song, and Stefano Ermon. 2021. Csd: Conditional score-based diffusion models for probabilistic time series imputation. *Advances in Neural Information Processing Systems* 34 (2021), 24804–24816.
- Tobii AB. 2023. *Tobii Eye Tracker 5*. Eye tracker for gaming. Available at: <http://gaming.tobii.com/product/eye-tracker-5/> (Accessed on: 21 March 2025).
- Rumeyza Turkmen, Zeynep Ecem Gelmez, Anil Ufuk Batmaz, Wolfgang Stuerzlinger, Paul Asente, Mine Sarac, Ken Pfeuffer, and Mayra Donaji Barrera Machuca. 2024. EyeGuide & EyeConGuide: Gaze-based Visual Guides to Improve 3D Sketching Systems. In *Proceedings of the 2024 CHI Conference on Human Factors in Computing Systems*. 1–14.
- Ashish Vaswani, Noam Shazeer, Niki Parmar, Jakob Uszkoreit, Llion Jones, Aidan N Gomez, Łukasz Kaiser, and Illia Polosukhin. 2017. Attention is all you need. *Advances in neural information processing systems* 30 (2017).
- Pauli Virtanen, Ralf Gommers, Travis E. Oliphant, Matt Haberland, Tyler Reddy, David Courmapeau, Evgeni Burovski, Pearu Peterson, Warren Weckesser, Jonathan Bright, Stéfan J. van der Walt, Matthew Brett, Joshua Wilson, K. Jarrod Millman, Nikolay Mayorov, Andrew R. J. Nelson, Eric Jones, Robert Kern, Eric Larson, C J Carey, Ilhan Polat, Yu Feng, Eric W. Moore, Jake VanderPlas, Denis Laxalde, Josef Perktold, Robert Cimrman, Ian Henriksen, E. A. Quintero, Charles R. Harris, Anne M. Archibald,

- Antônio H. Ribeiro, Fabian Pedregosa, Paul van Mulbregt, and SciPy 1.0 Contributors. 2020. SciPy 1.0: Fundamental Algorithms for Scientific Computing in Python. *Nature Methods* 17 (2020), 261–272. <https://doi.org/10.1038/s41592-019-0686-2>
- Hana Vrzakova, Mary Jean Amon, McKenzie Rees, Myrthe Faber, and Sidney D’Mello. 2021. Looking for a deal? visual social attention during negotiations via mixed media videoconferencing. *Proceedings of the ACM on Human-computer Interaction* 4, CSCW3 (2021), 1–35.
- Zhimin Wang, Jingyi Sun, Mingwei Hu, Maohang Rao, Weitao Song, and Feng Lu. 2024. GazeRing: enhancing hand-eye coordination with pressure ring in augmented reality. In *2024 IEEE International Symposium on Mixed and Augmented Reality (ISMAR)*. IEEE, 534–543.
- Katarzyna Wisiecka, Yuumi Konishi, Krzysztof Krejtz, Mahshid Zolfaghari, Birgit Kopainsky, Izabela Krejtz, Hideki Koike, and Morten Fjeld. 2023. Supporting complex decision-making: evidence from an eye tracking study on in-person and remote collaboration. *ACM Transactions on Computer-Human Interaction* 30, 5 (2023), 1–27.
- Haixu Wu, Tengge Hu, Yong Liu, Hang Zhou, Jianmin Wang, and Mingsheng Long. 2023. TimesNet: Temporal 2D-Variation Modeling for General Time Series Analysis. In *The Eleventh International Conference on Learning Representations*. https://openreview.net/forum?id=ju_Uqw384Oq
- Haodong Yan, Zhiming Hu, Syn Schmitt, and Andreas Bulling. 2024. GazeMoDiff: Gaze-guided Diffusion Model for Stochastic Human Motion Prediction. In *Proceedings of the 2024 Pacific Conference on Computer Graphics and Applications*.
- Brent Yi, Vickie Ye, Maya Zheng, Lea Müller, Georgios Pavlakos, Yi Ma, Jitendra Malik, and Angjoo Kanazawa. 2024. Estimating Body and Hand Motion in an Ego-sensed World. *arXiv preprint arXiv:2410.03665* (2024).
- Ailing Zeng, Muxi Chen, Lei Zhang, and Qiang Xu. 2023. Are Transformers Effective for Time Series Forecasting? *Proceedings of the AAAI Conference on Artificial Intelligence*.
- Guanhua Zhang, Zhiming Hu, and Andreas Bulling. 2024b. DisMouse: Disentangling Information from Mouse Movement Data. In *Proceedings of the 37th Annual ACM Symposium on User Interface Software and Technology*. 1–13.
- Mingyuan Zhang, Zhongang Cai, Liang Pan, Fangzhou Hong, Xinying Guo, Lei Yang, and Ziwei Liu. 2024a. Motiondiffuse: Text-driven human motion generation with diffusion model. *IEEE transactions on pattern analysis and machine intelligence* 46, 6 (2024), 4115–4128.
- Xucong Zhang, Yusuke Sugano, Mario Fritz, and Andreas Bulling. 2015. Appearance-based gaze estimation in the wild. In *Proceedings of the IEEE conference on computer vision and pattern recognition*. 4511–4520.
- Xucong Zhang, Yusuke Sugano, Mario Fritz, and Andreas Bulling. 2017. Mpiigaze: Real-world dataset and deep appearance-based gaze estimation. *IEEE transactions on pattern analysis and machine intelligence* 41, 1 (2017), 162–175.
- Yunhao Zhang and Junchi Yan. 2023. Crossformer: Transformer utilizing cross-dimension dependency for multivariate time series forecasting. In *The eleventh international conference on learning representations*.
- Zhaobo Zheng, Kumar Akash, Teruhisa Mitsu, Vidya Krishnamoorthy, Miaomiao Dong, Yuni Lee, and Gaojian Huang. 2022. Identification of adaptive driving style preference through implicit inputs in sae l2 vehicles. In *Proceedings of the 2022 International Conference on Multimodal Interaction*. 468–475.
- Haoyi Zhou, Shanghang Zhang, Jieqi Peng, Shuai Zhang, Jianxin Li, Hui Xiong, and Wancai Zhang. 2021. Informer: Beyond efficient transformer for long sequence time-series forecasting. In *Proceedings of the AAAI conference on artificial intelligence*, Vol. 35. 11106–11115.

A RESULT OF TIME-SERIES IMPUTATION BASELINES ON EGO-EXO4D AND HOT3D

We provide MAE of iTransformer [Liu et al. 2024], Dlinear [Zeng et al. 2023], TimesNet [Wu et al. 2023], BRITS [Cao et al. 2018] on the Ego-Exo4D [Grauman et al. 2024] and HOT3D [Banerjee et al. 2024] datasets in Table A.

	Ego-Exo4D				HOT3D			
	10%	30%	50%	90%	10%	30%	50%	90%
iTransformer [Liu et al. 2024]	7.89	11.04	17.55	26.36	6.81	9.83	15.80	24.46
DLinear [Zeng et al. 2023]	12.12	12.14	12.88	14.00	9.83	10.00	10.62	11.52
TimesNet [Wu et al. 2023]	21.66	20.27	22.37	25.23	19.83	18.79	20.51	23.23
BRITS [Cao et al. 2018]	10.51	12.47	14.96	19.17	9.47	11.36	13.50	17.20

Table 10. Mean angular error (MAE) of iTransformer [Liu et al. 2024], Dlinear [Zeng et al. 2023], TimesNet [Wu et al. 2023], BRITS [Cao et al. 2018] on the Ego-Exo4D [Grauman et al. 2024] and HOT3D [Banerjee et al. 2024] datasets.